Oxo- and Hydroxo-Bridged Diiron Complexes: A Chemical Perspective on a Biological Unit

DONALD M. KURTZ, JR.

Department of Chemistry, University of Georgia, Athens, Georgia 30602

Received October 1, 1989 (Revised Manuscript Received February 23, 1990)

Contents

Donald M. Kurtz, Jr., was born in Akron, OH, in 1950 and graduated with a B.S. degree in Chemistry from the University of Akron in 1972. In 1977 he received his Ph.D. degree in chemistry (majoring in physical biochemistry) at Northwestern University under Irving M. Klotz. He was a National Institutes of Health postdoctoral fellow under Richard H. Holm at Stanford University during 1977–1979. In 1979 he joined the faculty in the Department of Chemistry at Iowa State University. In 1986 he moved to the University of Georgia, where he is currently an Associate Professor of chemistry. Professor Kurtz is a National Institutes of Health Research Career Development Awardee during 1988–1993. His research interests involve the inorganic chemistry and biochemistry associated with non-heme iron proteins.

I. Introduction

The Fe–O–Fe linkage has been one of the more celebrated units in inorganic chemistry. Reasons for this phenomenon include its stability in the diferric form, its magnetic behavior, and its occurrence at the active centers of proteins. In 1974 Murray reviewed the chemistry of (μ-oxo)diiron(III) complexes.[1] While recent reviews are available on (μ-oxo)diiron sites in proteins,[2] no comprehensive summary focusing on the *chemistry* of the Fe–O–Fe unit has appeared in the interim. The present review *does* focus on the chemistry, hence the "chemical perspective" in the title.

Although several new complexes within the category of the title have appeared continually throughout the intervening period since 1974, a renaissance in this area began in 1983. A seminal contribution to this renewed activity was the synthesis of two μ-oxobis(μ-carboxylato)diiron(III) "hemerythrin site models" independently in the laboratories of Lippard[3] and Wieghardt.[4] As implied by the connection to hemerythrin, this renewed activity appears to be driven largely by attempts to understand the chemistry of an emerging group of diiron sites in proteins.

A. Limitations and Scope

One goal of this review is to collect the synthetic chemistry, spectroscopy, and magnetic behavior of the title complexes in a context that will provide a reference

0009-2665/90/0790-0585$09.50/0

frame for the biological sites. A second goal is to assess the advances that have been made in understanding the chemical nature of the Fe–O–Fe unit. A restriction to (μ-oxo)- and (μ-hydroxo)diiron molecular structures is imposed; linear chains and other extended arrays that occur in the solid state are not included. The restriction to oxo and hydroxo bridges emphasizes the importance of water and the biological connection to this chemistry. Reactions leading to iron complexes of higher nuclearity have recently been summarized[5] and are not included here. Compounds containing additional transition-metal atoms are excluded, unless the diiron complex is magnetically isolated. Since Murray's review was comprehensive, and included historical aspects, results obtained since 1972 are emphasized here. The literature is surveyed through at least mid-1989. Some aspects of the title topic have been covered in more general reviews.[5,6] A list of abbreviations is included at the end.

One is struck by the wealth of structural and spectroscopic information on the title complexes and conversely by the lack of information on reactivity. The former circumstance reflects attempts to understand the electronic and magnetic nature of these complexes as well as their use as spectroscopic points of reference for the biological sites. The lack of information on reactivity is most probably due to the great stability of the (μ-oxo)diferric unit under a variety of conditions. In fact one likely reason for the large number of these complexes (cf. Tables I and II) is that the Fe–O–Fe unit is difficult to avoid in ferric chemistry!

The oxo-bridged diiron complexes known at the time of the previous review were all diferric, and the vast majority of the complexes reported since 1972 are as well (Tables I and II). The relative instabilities of the mixed-valent and diferrous oxo/hydroxo-bridged complexes have limited their numbers. Only two $Fe^{II}Fe^{III}$ complexes and one diferrous complex within the title category have been reported as isolable salts by mid-1989. One structurally characterized example of a formally diiron(I) hydroxo-bridged complex is known. Mixed-valent $Fe^{III}Fe^{IV}$ complexes have been reported, but are ill-characterized. In this review, unless otherwise specified, the term "mixed-valent" refers specifically to the $Fe^{II}Fe^{III}$ oxidation level. Molecular formulas can be assumed to contain only Fe^{III} unless the oxidation states are specifically noted otherwise.

B. Hydrolysis of Fe(III)(aq)

The nature of the diiron(III) species that results from hydrolysis of Fe(III)(aq) at pH >1 was controversial in 1974 and still has not been resolved. The uncertainty is illustrated in two recent inorganic texts, one of which assigns a μ-oxo[7] and the other a bis(μ-hydroxo) structure[8] to the major diiron(III) species between pH 1 and 3. The two species in question may be related by equilibrium 1.[1] The uncertainty can be traced to the

$$H_2O + [(H_2O)_4Fe(\mu\text{-}OH)_2Fe(H_2O)_4]^{4+} \rightleftharpoons [(H_2O)_5Fe(\mu\text{-}O)Fe(H_2O)_5]^{4+} \quad (1)$$

heterogeneity of the hydrolyzed species and the dependence of the species distribution on conditions (temperature, concentration, salt, solvent etc.).[9-11] Furthermore, no diiron(III) species containing only aquo, hydroxo, and/or oxo ligands has ever been crystallized. An X-ray absorption experiment addressing this question[12] was shown to be in error.[13,14] Compounding the uncertainty is that either (μ-oxo)- or bis(μ-hydroxo)diiron(III) complexes, namely, $[Fe(H_2O)_2(Cl\text{-}dipic)]_2O\cdot 4H_2O$[15] and $[Fe(dipic)(H_2O)(OH)]_2$,[16] respectively, can be isolated from aqueous hydrolytic reactions of $FeCl_3\cdot 6H_2O$ in the presence of pyridinedicarboxylate ligands.

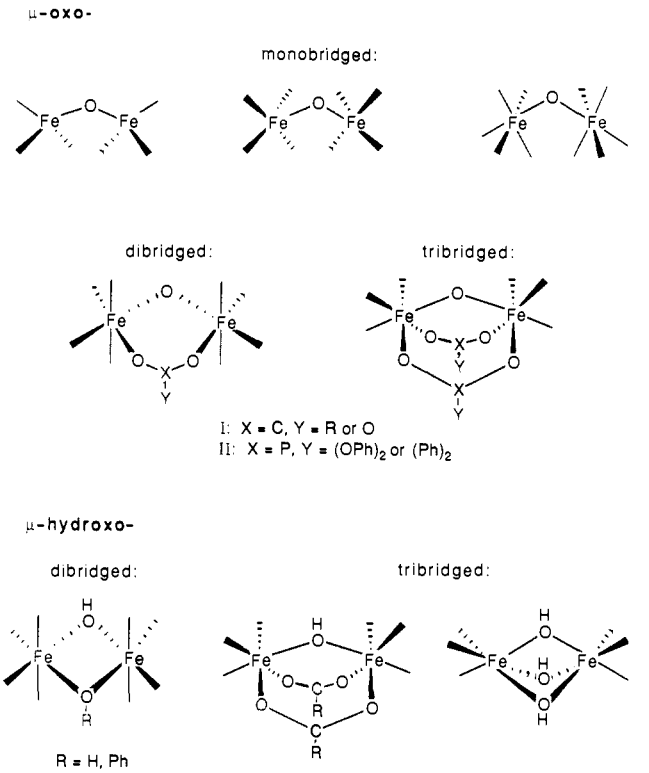

Figure 1. Schematic bridging structures of (μ-oxo/hydroxo)diiron complexes. Additional examples of μ-O_2XY groups are given in the text and tables.

II. Structure

A. Bridging Structural Types

Seven X-ray crystal structures containing the Fe–O–Fe unit were available for Murray's 1974 review, and these structures were all of the μ-oxo-monobridged type. More than 70 additional structures have been reported by mid-1989, and these include the structural types illustrated schematically in Figure 1. The known structures can be separated into μ-oxo and μ-hydroxo categories; aqua-bridged diiron complexes are unknown. In Figure 1 these two categories have each been subdivided into mono-, di-, and tribridged in the case of μ-oxo and di- and tribridged in the case of μ-hydroxo. Relevant structural parameters for these complexes are listed in Table I. These parameters have been obtained exclusively by X-ray crystallography. Where distances obtained by EXAFS have been compared to those obtained by X-ray crystallography, the agreement is found to be excellent for the first coordination sphere.[17,18] Fe···Fe distances obtained by EXAFS are subject to interference from outer shells of C and N scatterers, but agreement to within 0.04 Å is usual.

1. μ-Oxo Category

Within the μ-oxo category all known complexes save one (noted below) are diferric. The majority of the

μ-oxo complexes are of the monobridged type. It is noteworthy that prior to 1983 the tribridged subcategories were unknown outside of a protein. The dibridged (μ-oxo)(μ-carboxylato) structures have been even more recent entrants. Supporting bridges consist exclusively of oxygen-donor ligands. Coordination numbers of 4, 5, and 6 (and, possibly, a single example of 7)[1] are known. Within the monobridged subcategory a clear preference for 4-coordination is shown with halides (and one example of thiolate),[19] whereas 5- or 6-coordination is strongly preferred with chelating N- and O-donor ligands. The complex $[Fe_2O(N5)Cl_3]Cl\cdot 2C_2H_5OH$ illustrates the preceding two statements, showing both 4- and 6-coordination.[20] This 4,6 complex and the 5,6 complex, $[Fe(hp)]_2O(H_2O)$,[21] constitute the only examples of different coordination numbers in a single diiron μ-oxo/hydroxo complex.

Unusually short Fe–O(oxo) distances are characteristic of the diferric Fe–O–Fe unit. Fe–O(oxo) distances range from 1.73 to 1.82 Å, with the average being 1.77 Å. The average for the 4-coordinate complexes is somewhat shorter at 1.75 Å. These differences in length are nicely illustrated in the 4,6 complex mentioned above (Table I). The porphyrinato complexes may have slightly shorter than average Fe–O(oxo) bonds (~1.76 Å). The Fe–O–Fe angle in the μ-oxo complexes is quite flexible, ranging from 114° to 180°. The smallest known Fe–O–Fe angle in the monobridged subcategory is 139° in $[Fe(salen)]_2O\cdot(py)_2$.[22] The Fe···Fe distances are longer for the μ-oxo-monobridged complexes (3.39–3.56 Å) than for the di- and tribridged complexes (3.05–3.39 Å). The average Fe–O(oxo) distance increases from 1.78 Å in $[Fe(acen)]_2O$[23] to 2.03 Å in $\{Na[Fe^{II,III}(acen)]_2O\}_2$,[24] the latter of which is the only structurally characterized complex that contains a mixed-valent (μ-oxo)diiron unit. The oxo bridge in this mixed-valent complex may be stabilized by weak bonding to a sodium ion. The tetranuclear formulation is the result of Fe–O(oxo)···Na^+···O(acen)–Fe linkages between $Fe^{II}Fe^{III}$ pairs.

2. μ-Hydroxo Category

A single hydroxo bridge is by itself apparently incapable of holding two iron atoms together, since this bridge does not appear without "supports". With the exception of one organometallic compound (noted below), the supporting bridges consist of oxygen-donor ligands, and 6 is the only known coordination number. The bridging Fe–O distance lengthens to 1.96–2.06 Å, a range encompassing all oxidation levels. With two exceptions mentioned below, the Fe···Fe distances of the title complexes indicate that metal–metal bonding need not be considered. (This statement may not strictly apply to antiferromagnetic coupling, a point discussed elsewhere in this review.) For (μ-hydroxo)diferric complexes the Fe···Fe distances are shorter for dibridged (3.08–3.16 Å) than for tribridged (3.4 Å, only one example). Fe–O(H)–Fe angles range from 103° to 123°, with the bis(μ-hydroxo) complexes being at the lower end of this range. The exceptions are the organometallic complex $[Fe^I_2(CO)_6(btp)(OH)]$ and $\{[Fe^{II,III}(MTACN)]_2(OH)_3\}(ClO_4)_2\cdot 2CH_3OH\cdot 2H_2O$, with Fe–O(H)–Fe angles of 79°[25] and ~77°,[26] respectively. The former complex represents the only structural type not explicitly illustrated in Figure 1. $[Fe^I_2(CO)_6(btp)(OH)]$ has a dibridged (μ-hydroxo)(μ-phosphido) structure,

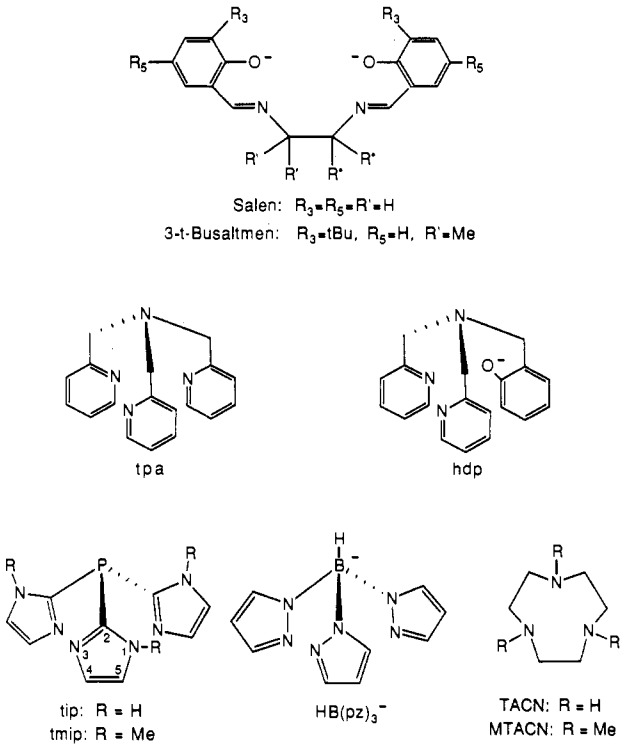

Figure 2. Examples of terminal ligands on mono- (salen), di- (tpa, hdp), and tribridged (tmip, $HB(pz)_3$, TACN) (μ-oxo)diiron complexes.

with terminal carbonyl ligands.[25] $\{[Fe^{II,III}(MTACN)]_2(OH)_3\}(ClO_4)_2\cdot 2CH_3OH\cdot 2H_2O$ is currently the only example of the tris(μ-hydroxo) structure.[26] These two complexes have unusually short Fe···Fe distances (~2.5 Å), and an Fe–Fe bond is likely in $[Fe^I_2(CO)_6(btp)(OH)]$.

B. Types of Terminal Ligands and Their Structural Effects

For 5-coordinate complexes in the μ-oxo-monobridged subcategory, nonbonded repulsion energies appear to outweigh any electronic preferences for a particular Fe–O–Fe angle.[27-29] Mukherjee et al.[27] have used steric repulsions of bulky R groups on the salen ligand (cf. Figure 2) in order to increase the Fe–O–Fe angle from 145° in $[Fe(salen)]_2O$ to 173° in $[Fe(3\text{-}t\text{Busaltmen})]_2O$, without significantly increasing the Fe–O(oxo) distances. The Fe–O–Fe angle and Fe–O(oxo) distance in the anion of $[FeCl(DMSO)_5][Fe_2OCl_6]$ are reported to change significantly with temperature in the crystal (cf. Table I).[134]

The structural trans effect of the oxo bridge is evident in most of the tribridged diferric complexes whose capping tridentate ligands have 3-fold rotational symmetry. Fe–N or Fe–O bonds that are trans to the oxo bridge are 0.03–0.08 Å longer than the cis Fe–N or Fe–O bonds in complexes with $HB(pz)_3$,[30] TACN,[4,31] MTACN,[32] $\{[OP(OEt)_2]_3Co(C_5H_5)\}^-$,[33] and tmip[34,35] as capping ligands. Schematic structures of $HB(pz)_3$, TACN, MTACN, and tmip are illustrated in Figure 2, and the X-ray crystal structure of $[Fe_2O(OAc)_2(tmip)_2](ClO_4)_2$ is shown in Figure 3. In this cluster the average trans Fe–N distance is 0.03 Å longer than the average cis Fe–N distance. This trans effect is also clearly evident in solution from the ^1H NMR chemical shifts of the ligand imidazolyl resonances.[34] For exam-

TABLE I. Selected Structural Details of Oxo- and Hydroxo-Bridged Diiron Complexes

complex[a]	coord no.	Fe–O,[b] Å	Fe–O–Fe,[b] deg	Fe···Fe,[c] Å	ref
		μ-Oxo Monobridged			
$[Fe(acen)]_2O$	5	1.775 (13)	150.7 (13)	3.433 (3)	23
$\{Na[Fe^{II,III}(acen)]_2O\}_2$	5	1.999 (6)	134.9 (4)	3.757 calc	24
		2.069 (6)			
$[Fe(3\text{-}t\text{Busaltmen})]_2O$	5	1.779 (5)	173.4 (2)	3.551	27
$[Fe(salen)]_2O$	5	1.78 (1)	144.6 (6)	3.391	121a
$[Fe(salNPhCl)]_2O$	5	1.76 (1)	175 (1)	3.53	121b
$[Fe(tsalen)]_2O\cdot py$	5	1.78 (1)	159 (2)	3.50 (1)	99
$\{[(TACN)Fe(acac))]_2O\}(ClO_4)$	5	1.787 (5)	158.6 (3)	3.512 (2)	122
$\{Fe[TAAB(OMe)_2]\}_2O$	5	1.777 (6)	176.3 (3)	3.552 (1)	123
$[Fe(DAPH)_2Fe_2OCl_4]\cdot 4CH_3OH$	4	1.766 (3)	155.4 (6)	3.451 calc	124
$(Ph_4As)_2[Fe_2OCl_6]$	4	1.74 (3)	170.8 (5)	3.469 calc	124
$[Mg(DMF)_6][Fe_2OCl_6]$	4	1.734 (1)	180	3.468 calc	125
$(Et_4N)_2[Fe_2O(SPh)_6]$	4	1.766 (2)	180	3.532 calc	19
$[(C_5H_5)_2Fe]_2[Fe_2OCl_6]$	4	1.757 (2)	162.4 (9)	3.460 (3)	126
		1.754 (2)	160.8 (7)	3.459 calc	127
		1.749 (4)	162.1 (5)	3.455 calc	128
$(BzPh_3P)[Fe_2OCl_6]$	4	1.760 (4)	160.2 (5)	3.467 (2)	129
$(BzMe_2PhN)_2[Fe_2OCl_6]$	4	1.766 (5)	147.7 (3)	3.393 (1)	130
$(NEtpy)_3[FeCl_4][Fe_2OCl_6]$	4	1.744	180	3.489	131
$[Fe^{II}(bipy)_3][Fe_2OCl_6]$	4	1.765 (3)	148.1 (2)	3.394 calc	132
	4	1.75 (11)	148.9 (7)	3.374 calc	133
$[FeCl(DMSO)_5][Fe_2OCl_6]$	4	103 K 1.776	146.5 (2)	3.401 calc	134
		343 K 1.736	152.7 (4)	3.374 calc	
$[Fe^{II}(phen)_3][Fe_2OCl_6]$	4	1.75 (2)	161.6 (9)	3.45 calc	135
$(pyH)_2[Fe_2OCl_6]\cdot py$	4	1.755 (3)	155.6 (7)	3.431 calc	136
$(Ph_4P)_2[Fe_2OCl_6]\cdot 2CH_2Cl_2$	4	1.740 (1)	180	3.480	137
$[(C_6H_5)_3P)_2Se]_2[Fe_2OCl_6]$	4	1.752 (2)	180.0 (0)	3.504	138
$[Cu(en)_2]_2Fe_2O(EDTA)_2]\cdot 2H_2O$	6	1.773 (5)	169.7 (2)	3.533 (1)	139
$[Fe(TPC)]_2O$	5	1.755 (5)	180	3.510 (8)	77
$[Fe(TPP)]_2O$	5	1.759 (1)	176.1 (2)	3.516 calc	140
$[Fe(ODM)]_2O$	5	1.752 (1)	178.6 (6)	3.504 calc	141
$[Fe(FF)]_2O\cdot H_2O\cdot 2C_6H_5CH_3$	5	1.787 (17)	161.1 (4)	3.525 calc	142
$[Fe(ambp)]_2O$	6	1.811 (1)	146.6 (2)	3.468 (1)	143
$[Fe_2O(N5)Cl_3]Cl\cdot 2C_2H_5OH$	4	1.751 (4)	149.8 (3)	3.412 (1)	20
	6	1.782 (4)			
$[Fe(hp)]_2O(H_2O)$	5	1.739 (7)	180	3.52	21
	6	1.782 (7)			
$[Fe(cpbN)]_2O\cdot C_8H_{10}$	6	1.806 (3)	144.5 (2)	3.440 calc	48
$[Fe_2O(phen)_4(H_2O)_2](NO_3)_4\cdot 5H_2O$	6	1.785 (5)	155.1 (4)	3.49	56
$[Fe_2O(phen)_2(H_2O)_6](NO_3)_4\cdot H_2O$	6	1.774 (4)	162.0 (3)	3.506 (2)	144
$[Fe_2O(phen)_4Cl_2]Cl_2\cdot 4.5H_2O$	6	1.787 (6)	161 (1)	3.52 calc	133
$[Fe(TDAD)]_2O\cdot 0.67DMF$	5	1.767 (9)	157 (1)	3.46 calc	145
$[Fe(DBAT)]_2O\cdot CH_3CN$	5	1.792 (1)	142.75 (9)	3.397 calc	146
$[Fe(H_2O)_2(Cl\text{-}dipic)]_2O\cdot 4H_2O$	6	1.772 (3)	180	3.545 (1)	15
$[Fe_2O(tetren)_2]I_4$	6	1.77 (1)	172	3.531 calc	147a
$[Fe(mhq)_2]_2O\cdot CHCl_3$	5	1.780 (11)	151.6 (7)	3.451 calc	148
$[Fe(DSIT)]_2O\cdot 2H_2O$	5	1.769 (3)	156.4 (2)	3.481 (4)	149
$[Fe_2O(bbimae)_2Cl_2](NO_3)_2$	6	1.7816 (7)	180	3.563 (1)	150
$[Fe_2O(bbimae)_2(NCS)_2](NO_3)_2$	6	1.7795 (8)	180	3.559 (1)	150
		μ-Oxo Dibridged			
$[Fe_2O(OBz)(hdp)_2]BPh_4$	6	1.79 (1)	128.3 (6)	3.218 (2)	38
$[Fe_2O(OBz)(tpa)_2](ClO_4)_3$	6	1.790 (5)	129.7 (3)	3.241 (1)	39
$[Fe_2O(OAc)(tpa)_2](ClO_4)_3\cdot 2H_2O$	6	1.795 (5)	129.2 (2)	3.243 (1)	39
$[Fe_2O\{O_2P(OPh)_2\}](ClO_4)_3$	6	1.80	138	3.36 calc	55
		μ-Oxo Tribridged			
$\{[Fe(tpbn)(OAc)]_2O\}_2(NO_3)_4\cdot 4H_2O$	6	1.794 (3)	121.3 (6)	3.129 (2)	37a
$[Fe_2O(OAc)_2(MTACN)_2](ClO_4)_2\cdot H_2O$	6	1.800 (3)	119.7 (1)	3.12 (4)	32
$[Fe_2O(OAc)_2Cl_2(bipy)_2]\cdot CH_3CN$	6	1.785 (4)	123.9 (2)	3.151 (1)	36
$[Fe_2O(OBz)_2(N3)_2](ClO_4)_2\cdot 2C_2H_5OH\cdot 0.5(Et_3NH)(ClO_4)$	6	1.790 (6)	118.7 (3)	3.079 (2)	49a
$[Fe_2O(OAc)_2(HB(pz)_3)_2]\cdot 4CH_3CN$	6	1.785 (2)	123.6 (1)	3.145 (1)	30
$[Fe_2O(O_2CH)_2(HB(pz)_3)_2]$	6	1.781 (3)	125.5 (2)	3.168 (1)	30
$[Fe_2O(O_2P(OPh)_2)_2(HB(pz)_3)_2]$	6	1.808 (3)	134.7 (2)	3.335 (1)	53, 54
$[Fe_2O(O_2PPh)_2)_2(HB(pz)_3)_2]$	6	1.812 (3)	130.6 (3)	3.292 (2)	53, 54
$[Fe_2O(OAc)_2(TACN)_2]I_2\cdot 0.5NaI\cdot 3H_2O$	6	1.78 (1)	118.3 (5)	3.064 (5)	4
$[Fe_2O(OAc)_2(TACN)_2]I_2\cdot 0.5CH_3CN$	6	1.781 (4)	118.7 (4)	3.063 (2)	31
$[Fe_2O(OAc)_2(tmip)_2](ClO_4)_2\cdot 2CH_3CN\cdot (C_2H_5)_2O$	6	1.800 (5)	122.7 (2)	3.158 (2)	35
$[Fe_2O(CO_3)_2(MTACN)]\cdot 4.25H_2O$	6	1.820 (8)	113.8 (4)	3.048 (2)	50
$[Fe_2O(OAc)_2\{[OP(OEt)_2]_3Co(C_5H_5)\}_2]$	6	1.795 (6)	124.4 (4)	3.174 (2)	33
$[Fe_2O(MPDP)(HB(pz)_3)_2]$	6	1.797 (4)	123.4 (3)	3.161 (1)	172
		1.793 (5)			
$[Fe_2O(MPDP)(4,4'\text{-}Me_2bipy)_2Cl_2]$	6	1.771 (3)	124.0 (2)	3.130 (1)	172
		1.774 (3)			
$[Fe_2O(MPDP)(BIPhMe)_2Cl_2]$	6	1.783 (5)	125.9 (2)	3.183 (2)	172
		1.790 (4)			

TABLE I (Continued)

complex[a]	coord no.	Fe–O,[b] Å	Fe–O–Fe,[b] deg	Fe···Fe,[c] Å	ref
$[Fe_2O(O_3P(OC_6H_5))_2(MTACN)_2]NaClO_4 \cdot 2H_2O$	6	1.817 (5)	123.2 (3)	3.198 (3)	174
$[Fe_2O(CrO_4)_2(MTACN)_2] \cdot 4H_2O$	6	1.819 (2)	129.1 (3)	3.285 (4)	174
		μ-Hydroxo Dibridged			
$[Fe_2(MeHXTA)(OH)(H_2O)_2] \cdot 4H_2O$	6	1.96 (2)	106.34 (17)	3.137 (1)	151, 152
$[Fe_2((sal)_3trien)(OH)Cl_2] \cdot C_4H_8O$	6	1.97 (1)	107 (1)	3.162 (7)	97
$[Fe_2(salam)(OH)_2] \cdot 2H_2O \cdot 2py$	6	1.986 (6) 2.055 (6)	102.8 (3)	3.155 (3)	98
$[Fe(Chel)(H_2O)(OH)]_2 \cdot 4H_2O$	6	1.938 (4) 1.989 (4)	103.2 (6)	3.078 (2)	16
$[Fe(dipic)(H_2O)(OH)]_2$	6	1.938 (5) 1.993 (5)	103.6 (2)	3.089 (2)	16
$[Fe(DMAdipic)(H_2O)(OH)]_2$	6	1.937 (6) 1.986 (9)	105.3 (2)	3.118 (2)	153
$[Fe^{I}_2(CO)_6(btp)(OH)]$	6	1.972 (6) av	79.1 (2)	2.511 (2)	25
		μ-Hydroxo Tribridged			
$[Fe^{II}_2(OH)(OAc)_2(MTACN)_2](ClO_4) \cdot H_2O$	6	1.987 (8)	113.2 (2)	3.32 (1)	52
$\{[Fe^{II,III}(MTACN)]_2(OH)_3\}(ClO_4)_2 \cdot 2CH_3OH \cdot 2H_2O$	6			2.509 (6)	26
$[Fe_2(OH)(OAc)_2(HB(pz)_3)_2](ClO_4) \cdot 0.5CH_2Cl_2$	6	1.956 (5)	123.1 (2)	3.439 (1)	51

[a] Formal iron oxidation states other than III are indicated. [b] Number in parentheses is the esd of a single value or the average esd of two values. [c] calc indicates that the distance was calculated trigonometrically.

ple, the cis N(1)–H resonance of $[Fe_2O(OAc)_2(tip)_2]^{2+}$ appears ~4 ppm farther downfield than does the trans N(1)–H resonance (cf. Table III). The shorter cis than trans Fe–N(Im) distances permit more unpaired electron spin to be delocalized onto the cis imidazolyl ring protons. In $[Fe_2O(OAc)_2\{[O_2P(OEt)_2]_3Co(C_5H_5)\}_2]$, the tribridged core is capped by the tripodal oxygen-donor ligand $\{[O_2P(OEt)_2]_3Co(C_5H_5)\}^-$. In this complex the Fe–O bonds trans to the oxo bridge are ~0.07 Å longer than the cis Fe–O bonds.[33] It is also noteworthy that, among these tridentate capping ligands, TACN forms the diferric (μ-oxo)bis(μ-carboxylato) complex with the shortest Fe···Fe distance (cf. Table I). The rationale for this observation is that the small size of TACN and the trigonal contraction that this ligand imposes on the coordination sphere reduce its steric interactions with the bridging ligands.[32]

The complex $[Fe_2O(OAc)_2Cl_2(bipy)_2] \cdot CH_3CN$[36] was the first example in the μ-oxo-tribridged category to contain other than a tridentate capping ligand. The terminal ligands on each iron instead consist of the bidentate ligand bipy and Cl^-. More recent examples of such complexes with bidentate terminal ligands are $[Fe_2O(MPDP)L_2Cl_2]$ where L = 4,4′-Me_2bipy, BIPhMe, TMICMe.[172] This latter set of complexes is apparently stabilized by use of the bridging dicarboxylate MPDP. In all of these complexes the Cl^- ligands are coordinated cis to the oxo bridge. $[Fe_2O(O_2CH)_4(BIPhMe)_2] \cdot H_2O$ contains the bidentate terminal ligand BIPhMe and a terminal formato ligand on each iron coordinated cis to the oxo bridge.[173]

Use of the potentially dinucleating ligands tptn, tbtn, and dtne[37] in syntheses of the μ-oxo-tribridged complexes failed to achieve the desired result, i.e., one diiron complex surrounded by one dinucleating ligand. Instead, tetranuclear cations were obtained that can be described as a "dimer of dimers". The cation consists of two linked but magnetically isolated tribridged diiron(III) subcomplexes, whose structures are analogous to that shown in Figure 3. The Fe–Fe axes of these two subcomplexes are oriented approximately parallel to each other. Each of two dinucleating ligands caps one end of both subcomplexes.

The dibridged (μ-oxo)(μ-carboxylato) structures in $[Fe_2O(OBz)(hdp)_2]BPh_4$[38] and $[Fe_2O(OBz)(tpa)_2](ClO_4)_3$[39] are apparently encouraged by use of the tetradentate capping ligands hdp and tpa whose schematic structures are shown in Figure 2. The tertiary amino nitrogens from which the other substituents emanate distinguish these tetradentate ligands from the salen type, which enforces a more planar coordination sphere. Identical environments for the two iron atoms are found in $[Fe_2O(OBz)(hdp)_2]BPh_4$, where the tertiary amino nitrogen ligands to each iron are trans to the oxo bridge.[38] However, distinctly different coordination environments are found for the two iron atoms in $[Fe_2O(OBz)(tpa)_2](ClO_4)_3$. On one iron atom the tertiary amino nitrogen is trans to the oxo bridge; on the other iron atom a pyridyl nitrogen is trans to the oxo bridge. This pyridyl Fe–N distance is significantly longer than the remaining pyridyl Fe–N distances in the complex; thus, the structural trans effect of the oxo bridge is also evident for the dibridged complexes. The reason for the two different coordination environments in $[Fe_2O(OBz)(tpa)_2](ClO_4)_3$ is not obvious. The same two coordination environments are seen in $[Fe_2O(OAc)(tpa)_2](ClO_4)_3$.[39]

III. Synthesis

A. General Methods

Two approaches to syntheses of the μ-oxo-monobridged complexes were summarized in Murray's review:[1] (i) hydrolysis of ferric chelate complexes or of ferric salts in the presence of a chelating ligand, and perhaps a general base, in either water or an organic solvent and (ii) oxidation (usually aerial) of ferrous complexes, usually in nonaqueous solvents. These two approaches remain valid for complexes in this subcategory. No clear preference for one approach over the other has emerged during the intervening years, and these methods will not be recounted here.

B. Equilibria and Pathways of Formation

Equilibrium constants K_D for reaction 2 have been measured by spectrophotometric and/or potentiometric

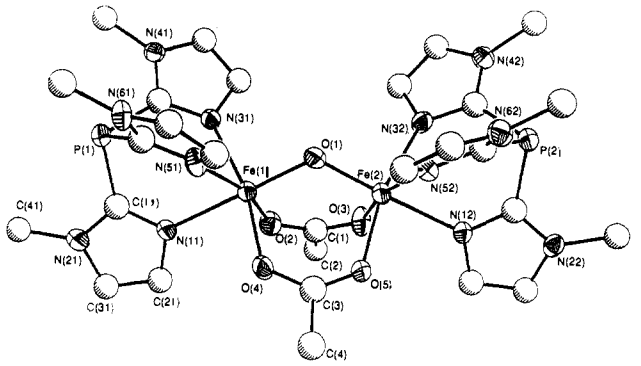

Figure 3. X-ray crystal structure of the diiron(III) complex in $[Fe_2O(OAc)_2(tmip)_2](ClO_4)_2 \cdot 2CH_3CN \cdot (C_2H_5)_2O$ (reprinted from ref 35; copyright 1990 American Chemical Society).

titrations with base in aqueous or mixed aqueous/organic solvents. $K_D \sim 10^{-12}$ M for L = salen and

$$2Fe^{III}L^+ + H_2O \overset{K_D}{\rightleftharpoons} (Fe^{III}L)_2O + 2H^+ \quad (2)$$

EDTA[40-42] and 10^{-8} M for L = TPP and TMpyP[43,44] at 25 °C. These values indicate that at neutral pH the equilibrium in reaction 2 favors the oxo-bridged species. While these values were not determined under identical conditions, the equilibrium does appear to lie further to the right for L = TPP than for L = salen or EDTA in aqueous solution. The reasons for this difference are not completely clear. Bulky groups on the phenyl rings of TPP can definitely lower K_D,[43] but additional factors, such as relative solvation of reactants vs products, must also be involved.[45] Relative insolubility of the oxo-bridged species in the reaction mixture is often an additional driving force for its formation. Intermediates in reaction 2 are not readily identifiable, although $Fe^{III}LOH$ is usually implicated.

Advances have been made in understanding the pathway(s) of formation of the (μ-oxo)diferric porphyrin complexes by reactions of ferrous porphyrins with O_2 in noncoordinating solvents.[46] Bulky substituents on the phenyl rings of TPP and use of low temperatures (<50 °C) hinder the formation of the μ-oxo species sufficiently so that intermediates can be detected in situ by ^{1}H NMR. The overall sequence of reactions involving identifiable intermediates is

$$PFe^{II} + O_2 \rightleftarrows PFe^{II}O_2 \overset{PFe^{II}}{\rightleftharpoons} PFe^{III}OOFe^{III}P \quad (3)$$

$$PFe^{III}OOFe^{III}P \rightarrow 2PFe^{IV}{=}O \quad (4)$$

$$PFe^{IV}{=}O + PFe^{II} \rightarrow PFe^{III}OFe^{III}P \quad (5)$$

The presence of N-bases favors formation of the ferryl species in reaction 4. At higher temperatures other pathways, such as those in reactions 6 and 7, leading

$$2PFe^{III}OOFe^{III}P \rightarrow PFe^{III}OFe^{III}P + O_2 \quad (6)$$

$$PFe^{III}OOFe^{III}P + 2PFe^{II} \rightarrow 2PFe^{III}OFe^{III}P \quad (7)$$

from the peroxo-bridged intermediate to the μ-oxo species may occur. Related oxygen atom transfer chemistry leading to (μ-oxo)diiron(III) complexes has been reviewed by Holm.[47] A reversible loss of the Fe–O–Fe linkage was reported upon heating of $[Fe(cpbN)]_2O$ in vacuo,[48] but the nature of the products is unknown.

Reduction of $[Fe(acen)]_2O$ by sodium in tetrahydrofuran produces $\{Na[Fe^{II,III}(acen)]_2O\}_2$, which is the only structurally characterized example of an oxo-bridged mixed-valent complex.[24]

C. Di- and Tribridged Complexes

The hydrolytic pathway of ferric salts at low pH involving an equilibrium analogous to reaction 1 presumably represents that for formation of the bis(μ-hydroxo) complexes such as $[Fe(dipic)(H_2O)(OH)]_2$.[16] The tribridged complexes represent a relatively recent development, and their syntheses deserve more detailed discussion.

Three synthetic routes to assembly of the diferric complexes in the μ-oxo-tribridged subcategory are given in reactions 8–10. Reaction 8 has been demonstrated

$$Fe(ClO_4)_3 \cdot 10H_2O + NaO_2CR \xrightarrow{H_2O} \xrightarrow{L^{0,-}} [Fe_2O(O_2CR)_2L]^{0,2+} \quad (8)$$

$$FeCl_3 \cdot 6H_2O + L \xrightarrow{EtOH} \text{“}LFeCl_3\text{”} \xrightarrow{O_2CR^-} [Fe_2O(O_2CR)_2L]^{2+} \quad (9)$$

$$(Et_4N)_2[Fe_2OCl_6] + Na_2O_2CR \xrightarrow{CH_3CN} \xrightarrow{L^{0,-}} [Fe_2O(O_2CR)_2L]^{0,2+} \quad (10)$$

for R = H, Me, or Et and L = $HB(pz)_3$, tmip, or tip.[30,32,35] Reaction 9 has been demonstrated for R = Me or Ph, and L = TACN, MTACN, tptn, tpbn, dtne, or N_3.[2,30,32,37,49a] Reaction 9 using (MTACN)$FeCl_3$ in water yields $[Fe_2O(\mu\text{-}X)_2L_2]$ when X = CO_3^{2-}, HPO_4^{2-}, $HAsO_4^{2-}$, or CrO_4^{2-} is used in place of O_2CR^-.[50,174] Reaction 10, which uses the preformed (μ-oxo)diiron(III) “synthon” $[Fe_2OCl_6]^{2-}$,[155] has been demonstrated for R = Me, Et, Ph and L = $HB(pz)_3$, tmip, or $\{[O_2P(OEt)_2]_3Co(C_5H_5)\}^-$.[30,33,35] Reaction 10 using the bridging dicarboxylate MPDP in place of Na_2O_2CR results in $[Fe_2O(MPDP)L_2Cl_2]$ where L = 4,4′-Me_2bipy, BIPhMe, or TMICMe.[172] The dibridged (μ-oxo)(μ-carboxylato) complexes $[Fe_2O(OBz)(hdp)_2]BPh_4$ and $[Fe_2O(OBz)(tpa)_2](ClO_4)_3$ have been prepared by a reaction similar to reaction 9 in methanol, but with tetradentate rather than tridentate capping ligands (cf. Figure 2).[38,39]

An alternative synthesis of the (μ-oxo)bis(μ-carboxylato)diiron(III) core involves splitting of the $[Fe_4(\mu_3\text{-}O)_2]^{8+}$ core in $[Fe_4O_2(OAc)_7(bipy)_2]^+$ in the presence of bipy and Cl^- to yield $[Fe_2O(OAc)_2Cl_2(bipy)_2] \cdot CH_3CN$.[36] Syntheses of $[Fe_2O(OAc)_2L'_]^{2+}$ (L′ = tptn, tbpn,[37] bbima[49b]) have been reported from reaction of L′ with “basic iron acetate”, which contains the trinuclear structure shown in Figure 8 with M = Fe^{3+} and L = H_2O. Aerial oxidation of a solution of $[Fe^{II}_2(O_2CH)_4(BIPhMe)_2]$ results in $[Fe_2O(O_2CH)_4(BIPhMe)_2] \cdot H_2O$.[173]

The (μ-hydroxo)bis(μ-carboxylato)diiron(III) complexes $[Fe_2(\mu\text{-}OH)(O_2CR)_2L_2]^{+,3+}$ have been obtained for L = $HB(pz)_3$ or tmip, and R = Me or Et.[34,35,51]

These hydroxo-bridged complexes are prepared either by protonation of the oxo-bridged complex in organic solvent or by reaction 8 carried out at pH $\lesssim$3.5. In the case of L = tmip, highest yields of the μ-hydroxo complex are obtained in the range pH 1.5–2.0.[35] Based on the pHs required for syntheses of the (μ-oxo)- vs (μ-hydroxo)bis(μ-carboxylato)diiron(III) complexes, a pK_a $\sim$3.5 for the diferric μ-hydroxo group has been estimated.[32]

The "spontaneous self-assembly" of the (μ-oxo)bis(μ-carboxylato)diiron(III) core with a variety of carboxylato ligands, capping ligands, and reaction conditions demonstrates the thermodynamic stability of this core. The major side products are the bis(ligand) complexes $Fe^{III}L_2$, which often have even greater thermodynamic stabilities. Suppression of this side product can be achieved by rapid removal of $[Fe_2O(O_2CR)_2L_2]^{0,2+}$ from the reaction mixture, usually by precipitation as it forms. In the case of L = MTACN the steric bulk of the methyl groups also suppresses formation of $Fe^{III}L_2$.

The stabilities of the corresponding ferrous bis(ligand) complexes apparently prevent obtainment of the (μ-hydroxo)bis(μ-carboxylato)diiron(II) complexes with L = $HB(pz)_3$, tmip, or TACN. However, steric hindrance of the methyl groups on MTACN suppresses formation of $Fe^{II}L_2$ sufficiently to permit spontaneous self-assembly of $[Fe^{II}_2(OH)(OAc)_2(MTACN)_2](ClO_4)\cdot H_2O$, which is the only known differous hydroxo-bridged complex. This complex forms in a methanolic mixture of ferrous perchlorate hexahydrate, MTACN, and acetate under anaerobic conditions.[52] The only structurally characterized example of a hydroxo-bridged mixed-valent diiron complex, $\{[Fe^{II,III}(MTACN)]_2(OH)_3\}(ClO_4)_2\cdot 2CH_3OH\cdot 2H_2O$, is prepared similarly, but without acetate.[26]

D. Bridge Substitution and Exchange

Diphenylphosphato- and diphenylphosphinato-bridged analogues $[Fe_2O(O_2P(OPh)_2)(HB(pz)_3)_2]$ and $[Fe_2O(O_2P(Ph)_2)_2(HB(pz)_3)_2]$ have been prepared by additions of the respective conjugate acids to solutions of $[Fe_2O(OAc)_2(HB(pz)_3)_2]$ in dichloromethane.[53,54] This bridge substitution reaction is an exploitation of the facile exchange of the bridging carboxylato ligands that occurs for these complexes in the presence of a proton donor.[5,30] The bridge substitution reaction in water of $[Fe_2O(OAc)_2(MTACN)_2]^{2+}$ with $O_3P(OC_6H_5)^{2-}$ leads to $[Fe_2O(O_3P(OC_6H_5))_2(MTACN)_2]$.[174] In this case the substitution takes place after dissociation of one of the bridging acetato ligands at alkaline pH. The resulting (μ-oxo)(μ-acetato)diiron(III) species reacts with $O_3P(OC_6H_5)^{2-}$. The oxo bridge of $[Fe_2O(O_2CR)_2L]^{0,2+}$ rapidly exchanges with labeled oxide from water that is added at 1–2 vol % in nonprotic solvents.[30,31,55] For μ-oxo-monobridged complexes, this procedure sometimes results in decomposition and the bridge must instead be labeled by assembly of the complex in $H_2{}^{18}O$.[56,57]

IV. Electronic Absorption Spectra

A. Survey

The (μ-oxo)diiron(III) complexes constitute the only category where absorption spectra have been analyzed in detail. The characteristic spectra of these complexes are discussed below. Unlike the diferric Fe–O–Fe unit, no characteristic spectrum has yet been identified for the diferric Fe–O(H)–Fe unit. A single broad absorption with λ_{max} at 375 nm (ϵ_{2Fe} = 9500 M^{-1} cm^{-1}) is reported for the near-UV spectrum of the (μ-hydroxo)bis(μ-carboxylato) complex $[Fe_2(OH)(OAc)_2(HB(pz)_3)_2](ClO_4)\cdot 0.5CH_2Cl_2$.[51] However, the analogous complex $[Fe_2(OH)(OAc)_2(tmip)_2](ClO_4)_2BF_4$ shows only a weak shoulder in this region.[35] The diferrous complex $[Fe_2(OH)(OAc)_2(MTACN)_2](ClO_4)_2\cdot H_2O$ is nearly colorless; its absorption spectrum has not been analyzed. Ligand field transitions of the diferrous site in hemerythrin have been analyzed.[58]

B. (μ-Oxo)diiron(III) Complexes

The electronic transitions of these complexes have most recently been assigned from analyses of absorption and CD spectra, polarized single-crystal spectra, and Raman excitation profiles. While a self-consistent picture emerges, it is probably fair to say that the assignments, particularly those of the bands in the region of 400–530 nm, cannot be considered definitive at this time.

1. Oxo Dimer Region

For the diferric complexes, Table II lists electronic absorption bands between 300 and 400 nm, the so-called oxo dimer region.[59] Based on analysis of the spectrum of $enH_2[(FeHEDTA)_2O]\cdot 6H_2O$, the diferric oxo dimer bands were originally assigned to combinations of ligand field transitions, referred to as simultaneous pair excitations.[1,60] Although the sums of ligand field transition energies come close to those in the oxo dimer region for $enH_2[(FeHEDTA)_2O]\cdot 6H_2O$, the corresponding match in energies is not good for the tribridged complexes. A convincing alternative case has been made by Reem et al.[59] that the absorptions in the oxo dimer region arise from oxo $\rightarrow$ Fe CT transitions. Figure 4 contains a diagram of the orbitals on the bridging oxo and iron atoms that Reem et al. propose to be involved in these transitions at various bridge angles. According to this model the highest energy band at all angles arises from oxo $p_z \rightarrow$ Fe d_{z^2} CT of σ symmetry. The energy of this band would lie well below 300 nm and has not been observed, probably due to intense overlapping absorbance by other groups in these complexes. The next lowest energy transition for the linear geometry arises from the oxo p_x,$p_y \rightarrow$ Fe d_{xz},d_{yz} CT of π symmetry, and this transition is degenerate. As the bridge angle departs from linearity, this transition splits and simultaneously the oxo $p_z \rightarrow$ Fe $d_{x'z}$ CT transition becomes allowed. Thus, for bent Fe–O–Fe geometries three π-derived transitions are expected. These transitions are indicated by stars in Figure 4. For $enH_2[(FeHEDTA)_2O]\cdot 6H_2O$ (Fe–O–Fe = 165°),[61] two absorption bands between 300 and 400 nm have been assigned to the two lower energy π-derived transitions and a peak at 285 nm has been assigned to the highest energy π-derived transition.[59] For the di- and tribridged complexes the highest energy π-derived transition may merge with the next lowest energy π-derived transition due to the more acute Fe–O–Fe angles (114–130°), as depicted in Figure 4C. Thus, two bands in the 300–400-nm region are assigned to these π-derived transi-

TABLE II. Some Magnetic and Spectroscopic Properties of Oxo- and Hydroxo-Bridged Diiron Complexes

complex[a]	μ_{eff}, μ_B ($-J$,[b] cm^{-1})	ν(Fe–O–Fe), cm^{-1} s	ν(Fe–O–Fe), cm^{-1} as	oxo dimer: λ, nm (ϵ, M^{-1} cm^{-1})[c]	δ_{Fe},[d] mm/s (ΔE_A)	ref
			μ-Oxo Monobridged			
$[Fe(acen)]_2O$	1.80		840			23
$[Na[Fe^{II,III}(acen)]_2O]_2$	3.64		780			24
$[Fe(salen)]_2O$	1.83 (89–92)		832			27, 91
$[Fe(3\text{-}t\text{Busaltmen})]_2O$	1.88 (100)			340 sh (12300) 380 sh (10200)		27
$[Fe(5\text{-}t\text{Busalen})]_2O$				344 (11000) 388 sh (9500)		27
$[Fe(tsalen)]_2O\cdot py$	1.89		792		0.43 (1.10) [4.2 K]	99
$[[(TACN)Fe(acac)]_2O](ClO_4)$	2.24 (89)		820–840	350 (3400) 398 (1700)		122
$[Fe[TAAB(OMe)_2]]_2O$	1.65 (118)		840			123c
$[[Fe(TAAB)]_2O](NO_3)_4\cdot 4H_2O$	1.77 (111)		810			123c
$[[Fe(TAAB)]_2O](ClO_4)_4\cdot 4H_2O$	2.33 (65)		810			123c
$(Ph_4As)_2[Fe_2OCl_6]$			840			124
$[Mg(DMF)_6][Fe_2OCl_6]$	1.68 [77 K]		870			125
$[(C_5H_5)_2Fe]_2[Fe_2OCl_6]$	2.22		853		0.24 (1.20) [300 K]	126
$[Fe^{II}(bipy)_3][Fe_2OCl_6]$	(134)		850		0.23 (1.22) [290 K]	154, 171
$[R_4N,R_4P)[Fe_2OCl_6]$[e]	1.71–1.74 (146)	454–463	843-883		0.22–0.23 (1.20–1.27) [300 K]	75, 129, 130, 155–157, 171
$(pyH)_2[Fe_2OCl_6]\cdot py$	1.94 (92) (127)	458	860–870		0.20 (1.26) [rt] 0.23 (1.22) [290 K]	57, 136 171
$(Ph_4P)_2[Fe_2OCl_6]$			875		0.29 (1.23) [202 K]	137
$[(C_6H_5)_3P)_2Se]_2[Fe_2OCl_6]$	(190)		832		0.23 (1.22) [290 K]	138, 171
$(BzPh_3P)_2[Fe_2OBr_6]$			830		0.22 (1.37) [300 K]	129
$(BzPh_3P)_2[Fe_2OI_6]$			835		0.22 (1.42) [300 K]	129
$[Cu(en)_2][Fe_2O(EDTA)_2]\cdot 2H_2O$	(85)					139
$[FeCl_2(OPPh_3)]_2O$	3.05 (42)		892			158
$[Fe(Pc)]_2O$						
(1)	2.10 (120)		854-820		0.37 (0.44) [4.2 K]	84, 85, 159
(2)	1.38–1.42 (195)				0.26 (1.25) [4.2 K]	84
$[(N\text{-base})PcFe]_2O$	1.86–2.16 (5.6–6.3)				0.17–0.20 (1.58-1.76) [300 K]	90
$[Fe(Sq)(H_2O)_2]_2O$	1.88 (96)		750–820		0.32 (0.67) [300 K]	168a
$[Fe(hp)]_2O(H_2O)$	2.09		878		0.39 (1.66) [78 K]	21, 170
$[Fe(DPDME)]_2O$	(122-146)	416	842–886 (tentative)			79, 160
$[Fe(TPP)]_2O$	1.86 (132-136)		876		0.41 (0.67) [4.2 K]	77, 78
$[Fe(TPC)]_2O$	1.84 (129)		867		0.40 (0.70) [4.2 K]	77
$[Fe(TPP(4\text{-}OCH_3))]_2O$	(147)					75
$[Fe(TPP(4\text{-}CF_3)]_2O$	(136)					75
$[Fe(TPP(F_5)]_2O$	(146)					75
$[Fe(ODM)]_2O$	1.9				0.39 (0.52) [78 K]	141
$[Fe(FF)]_2O$	(108)		845			142
$[Fe(OEP)]_2O$			790–870			164
$[Fe_2O(N5)Cl_3]Cl\cdot 2C_2H_5OH$	1.59 (125)	425	850			20, 55
$[Fe_2O(phen)_4(H_2O)_2](NO_3)_4$		395	827	350 (~8000)		56
$[Fe(DBAT)_2]O\cdot CH_3CN$	1.96					146
$[Fe(Cl\text{-}dipic)]_2O\cdot 4H_2O$	1.91 (107) [270 K]					15
$[Fe_2O(tetren)_2]I_4$	1.95 (98)					147b
$[Fe_2O(tetpy)_2](SO_4)_2$	(83)		832		0.66 (1.79) [rt]	161, 162
$[Fe_2O(bmem)_2](SO_4)_2$	(89)		828–840	360 sh (7000) 318 (10600)	0.71 (1.41)	161, 162
$[Fe_2O(phen)_4(NCS)_2](NCS)_2$	1.79		830		0.50 (1.43) [77 K]	163
$[Fe(PBZ)_2(SO_4)]_2\cdot 17H_2O$	2.11		825			165
$[Fe(mhq)_2]_2O\cdot CHCl_3$	2.12 (80)					148
$[Fe_2O(bipy)](SO_4)_2\cdot 5H_2O$	1.85 (101)		772-778?			95
$[Fe_2O(phen)](SO_4)_2\cdot 6H_2O$	1.85 (100)		772-778			95
$[Fe_2O(n\text{-}propsal)_4]$		409	838			55
$[Fe(DSIT)]_2O\cdot 2H_2O$	1.87 (98.6)				0.60 (0.78) [300 K]	166
$[Fe(TPPC)]_2O$	2.00		863			104
$[Fe_2O(bbimae)_2Cl_2](NO_3)_2$	1.81 (103)		841		0.40 (1.23) [295 K]	150
$[Fe_2O(bbimae)_2(NCS)_2](NO_3)_2$	1.82 (95-105)		833		0.40 (1.16) [295 K]	150
$[Fe(cpbN)]_2O\cdot C_8H_{10}$	2.20 (80)					48
$[Fe_2O(TACN)_2(N_3)_4]\cdot H_2O$	(76)		800	398 (3800)		167
$[Fe_2O(TACN)_2(SCN)_4]$	(75)		810	398 (18000)		167
$[Fe_2^{III,IV}O(salen)_2]PF_6$, ? ClO_4,BF_4,I_3	3.8-4.5 (7-12)				0.411 (1.24–1.54) [4.2 K]	91
$[Fe_2^{III,IV}O(TPP)_2]PF_6$,$BF_4$?	4.2–4.3 (82-119)				0.35 (1.24) [4.2 K]	91
			μ-Oxo Dibridged			
$[Fe_2O(OBz)(hdp)_2]BPh_4$		494	763		0.49 (1.40)	38, 55
$[Fe_2O(OBz)(tpa)_2](ClO_4)_3$	(118)	497	772	330 (~14000)	0.45 (1.40) [4.2 K]	39, 55
$[Fe_2O(OAc)(tpa)_2](ClO_4)_3\cdot 2H_2O$		499	770		0.45 (1.45) [4.2 K]	39, 55
$[Fe_2O[O_2P(OPh)_2](tpa)](ClO_4)_3$		454	778			39, 55
			μ-Oxo Tribridged			
$[[Fe(tpbn)(OAc)]_2O]_2(ClO_4)_4\cdot 4H_2O$	1.76	525	727	348 (7360)	0.48 (1.27) [4.2 K]	37a, 55
$[[Fe(tptn)(OAc)]_2O]_2(ClO_4)_4\cdot 4H_2O$	1.70 (120)	540	725	344 (10600)	0.48 (1.39) [4.2 K]	37a, 55

TABLE II (Continued)

complex[a]	μ_{eff}, μ_B ($-J$,[b] cm^{-1})	ν(Fe–O–Fe), cm^{-1} s	as	oxo dimer: λ, nm (ϵ, M^{-1} cm^{-1})[c]	δ_{Fe},[d] mm/s (ΔE_A)	ref
$[[Fe(dtne)(OAc)]_2O]Br_4 \cdot 2H_2O$				322 (6800)		37b
$[Fe_2O(OAc)_2(MTACN)_2](ClO_4)_2 \cdot H_2O$	(129)					32
$[Fe_2O(OAc)_2(MTACN)_2](PF_6)_2$		537		345 (10500)	0.47 (1.50) [4.2 K]	32, 55
$[Fe_2O(OAc)_2(TACN)_2]I_2$	1.84	540	749	333 (7360) 368 sh	0.46 (1.72)	4, 31, 32, 55
$[Fe_2O(OAc)_2Cl_2(bipy)_2]$	1.75 (132)			329 (6060)	0.37 (1.80) [120 K]	36
$[Fe_2O(OBz)_2(N3)_2](ClO_4)_2$	117	537	745	355 (4000)		49a, 55
$[Fe_2O(OAc)_2(N3)_2](ClO_4)_2$	118					49a
$[Fe_2O(OAc)_2(bbmia)_2](ClO_4)_2$	1.67 (117)	530–540	740–750			49b
$[Fe_2O(O_2P(OC_6H_5)_2)_2(HB(pz)_3)_2]$	1.87 (98)	478	767	320 (10300) 366 (9260)	0.53 (1.60)	53 54
$[Fe_2O(O_2P(C_6H_5)_2)_2(HB(pz)_3)_2]$	1.87 (93)	480		317 (7360) 361 (6320)	0.50 (1.57)	53, 54
$[Fe_2O(OAc)_2(HB(pz)_3)_2]$	1.71 (121)	528	751	339 (9270) 358 sh	0.52 (1.60) [4.2 K]	30, 55
$[Fe_2O(O_2CH)_2(HB(pz)_3)_2]$		525		342 (10200)		30
$[Fe_2O(OBz)_2(HB(pz)_3)_2]$		526		336 (9000)		30
$[Fe_2O(OAc)_2(tmip)_2](ClO_4)_2 \cdot CH_3CN \cdot (C_2H_5)_2O$	(120)			338 (7900) 360 sh (6900)	0.51 (1.64) [100 K]	35
$[Fe_2O(OPr)_2(tmip)_2](PF_6)_2$		533	749		0.52 (1.61) [4.2 K]	35, 55
$[Fe_2MgO(OAc)_6(py)_3]$	~2.4 (62)					69
$[Fe_2O(CO_3)_2(Me_3TACN)] \cdot 4.25H_2O$	(91)			340 (4000) 365 sh		50
$[Fe_2O(OAc)_2[[OP(OEt)_2]_3Co(C_5H_5)]_2]$	(109)	510		357 (13200)	0.56 (1.78) [4.2 K]	33
$[Fe_2O(O_2CH)_4(BIPhMe)_2 \cdot H_2O$		518		329 (6800) 354 sh (5800)	0.54 (1.81) [4.2 K]	173
$[Fe_2O(MPdP)(HB(pz)_3)_2]$		526		341 (4600)	0.53 (1.66) [4.2 K]	172
$[Fe_2O(MPDP)(4,4'\text{-}Me_2bipy)_2Cl_2]$	(119)	532		328 sh 365 sh	0.51 (1.66) [4.2 K]	172
$[Fe_2O(MPDP)(BIPhMe)_2Cl_2]$	(122)	522		341 (6000) 360 sh	0.54 (1.78) [4.2 K]	172
$[Fe_2O(O_3P(OC_6H_5))_2(MTACN)_2] \cdot NaClO_4 \cdot 2H_2O$	(98)		694	332 (7030) 355 sh		174
$[Fe_2O(CrO_4)_2(MTACN)_2] \cdot 4H_2O$	(124)		700	354 (9700) 374 (10000)		174
$[Fe_2O(HPO_4)_2(MTACN)_2] \cdot 3H_2O$	(80)		706	330 (7400) 360 (6500)		174
$[Fe_2O(HAsO_4)_2(MTACN)_2] \cdot 3H_2O$	(70)		702	333 (4300)		174
		μ-Hydroxo Dibridged				
$[Fe_2(MeHXTA)(OH)(H_2O)_2] \cdot 4H_2O$	5.07 (12)				0.50 (0.60) [4.2 K]	151
$[Fe_2((sal)_3trien)(OH)Cl_2] \cdot C_4H_8O$	(7.4)					97
$[Fe_2(salam)(OH)_2] \cdot 2H_2O \cdot 2py$	5.17 (10.4)	880[f]			0.49 (0.561) [4.3 K]	98
$[Fe(Sq)(OH)(H_2O)_2]_2 \cdot 2H_2O$	5.29 (6.9)	850			0.40 [300 K]	168a,c
$[Fe(Sq)(OH)(py)_2]_2 \cdot 2H_2O$	5.22 (8.0)	~850			0.41 (0.58) [300 K]	168a,b
$[Fe(Sq)(OH)(4\text{-}Mepy)_2]_2 \cdot 2H_2O$	5.19 (8.6)	~850			0.33 (0.55) [300 K]	168a,b
$[Fe(Sq)(OH)(3\text{-}Mepy)_2]_2 \cdot 2H_2O$	5.24 (7.8)	~850			0.40 (0.53) [300 K]	168a,b
$[Fe(dmg)_2(OH)]_2$	4.28	960			0.54 (0.70) [300 K]	169
$[Fe(sal)_2(OH)]_2$	4.13	960			0.63 (0.97) [300 K]	169
$[Fe(hmb)_2(OH)]_2$	4.03	960			0.69 (0.72) [300 K]	169
$[Fe(Chel)(H_2O)(OH)]_2 \cdot 4H_2O$	5.24 (7.3)	~900				153
$[Fe(dipic)(H_2O)(OH)]_2$	4.86 (11.4)	~900				153
$[Fe(DMAdipic)(H_2O)(OH)]_2$	4.94 (11.7)					16
		μ-Hydroxo Tribridged				
$[Fe_2(OH)(OAc)_2(HB(pz)_3)_2] \cdot (ClO_4) \cdot 0.5CH_2Cl_2$	4.36 (17)				0.47 (0.25)	51
$[Fe_2(OH)(OPr)_2(tmip)_2](ClO_4)_3$					0.45 (0.56) [100 K]	35
$[Fe^{II}_2(OH)(OAc)_2(MTACN)_2] \cdot (ClO_4) \cdot H_2O$	(13)				1.16 (2.83)	32, 52
$[[Fe^{II,III}(MTACN)]_2(OH)_3] \cdot (ClO_4)_2 \cdot 2CH_3OH \cdot 2H_2O$	10.5 per Fe_2				0.74 (~2)	26

[a] Iron oxidation states other than III are indicated. [b] μ_{eff} per Fe at or near 300 K unless otherwise indicated. $-J$ conventions are defined in the text. [c] Molar extinction coefficients per Fe–O–Fe unit. Cf. references for solvents. [d] Isomer shifts are relative to metallic iron at 300 K. A few values have been corrected from a sodium nitroprusside reference by subtraction of 0.257 mm/s. Temperature of the measurement, when known, is listed next to each value. [e] Data for several tetraalkyl/arylammonium and -phosphonium salts are combined. [f] For bis(μ-hydroxo)complexes, frequencies for the $Fe(OH)_2Fe$ deformation are listed.

tions for the di- and tribridged complexes. Figure 5 depicts absorption spectra for three of the (μ-oxo)bis(μ-carboxylato)diiron(III) complexes; the two bands in the 300–400-nm region are not always clearly resolved.

2. Lower Energy Bands

A pair of absorption bands at 440–460 and 480–510 nm with 5- to 10-fold lower intensities than those in the oxo dimer region are also observed in all of the (μ-oxo)bis(μ-X)diiron(III) complexes, including those with X = carboxylato,[30,31,35,172,173] carbonato,[50] phosphinato,[54] phosphato[54,174] arsenato,[174] and chromato.[174] The spectra of Figure 5 show these two bands for three of the (μ-oxo)bis(μ-carboxylato) complexes. These bands are also observed in spectra of the dibridged (μ-oxo)-(μ-carboxylato) complexes.[39] Clearly these bands are

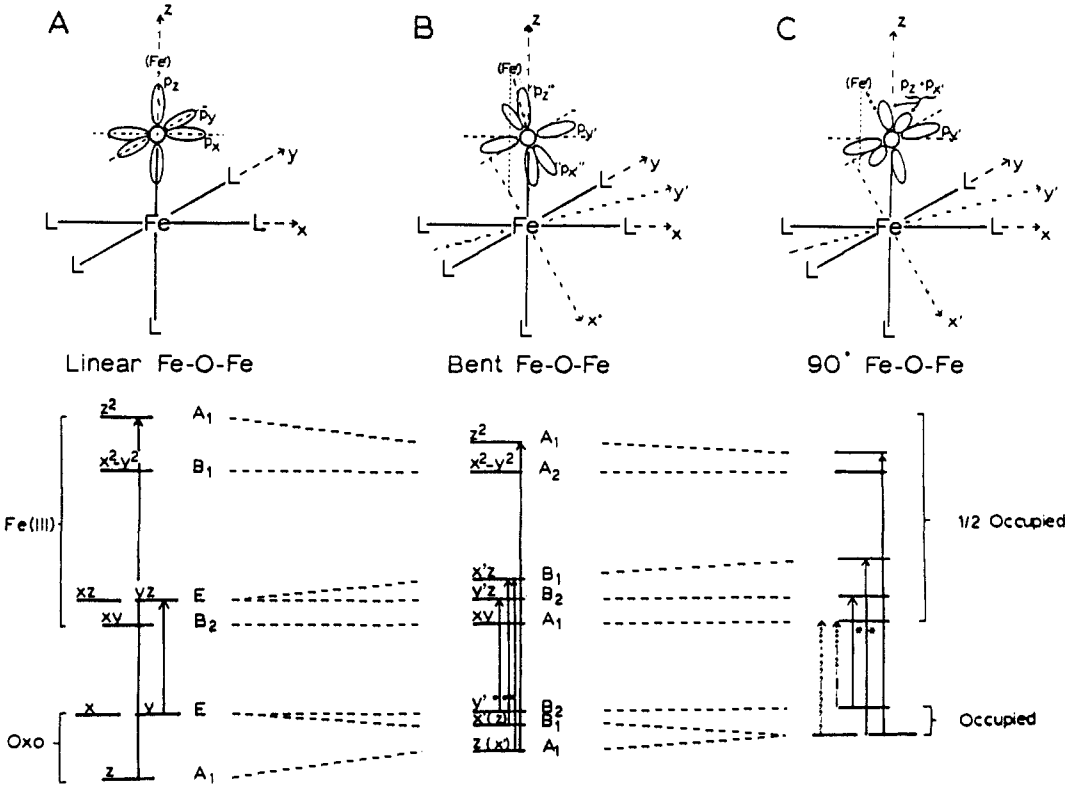

Figure 4. Schematic energy level diagram and illustrations of orbitals proposed to be involved in oxo → Fe CT transitions for oxo-bridged diiron(III) complexes (reprinted from ref 59; copyright 1989 American Chemical Society).

TABLE III. ^{1}H NMR Chemical Shifts at 300 K of Bridging Acetato and Terminal Imidazole Ligands in Tribridged High-Spin Ferric Complexes[a]

complex	μ_{eff}/Fe,[b] μ_B	$-J$,[c] cm^{-1}	δ_{OAc},[d] ppm	$\delta_{N(1)-H}$, ppm
$[Fe_2O(OAc)_2(t(m)ip)_2]^{2+}$	1.66	120	10.2	19.2 (cis) 15.7 (trans)
$[Fe_2MgO(OAc)_6(Im)_3]$	2.39	62	13.4[e]	20.6[f]
$[Fe_3O(OAc)_6(Im)_3]^+$	3.34	30	30.7[g]	35.3[h]
$[Fe_2(OH)(OAc)_2(t(m)ip)_2]^{3+}$	4.31	~17	66	85–100

[a] From refs 34 and 35. [b] Effective magnetic moments per iron atom at ~300 K determined by the Evans method. tmip (not tip) complexes were used. [c] Values are listed for the $\hat{H}_{ex} = -2JS_1 \cdot S_2$ formalism. Values for $[Fe_2MgO(OAc)_6(Im)_3]$ and $[Fe_3O(OAc)_6(Im)_3]^+$, respectively, are assumed to be the same as for py[69] and H_2O[71] in place of Im. [d] Chemical shifts of acetates that bridge two iron atoms. [e] For $[Fe_2MgO(OAc)_6(py)_3]$. [f] For $[Fe_2MgO(O_2CPh)_6(Im)_3]$. [g] For $[Fe_3O(OAc)_6(N\text{-MeIm})_3]^+$. [h] For $[Fe_3O(O_2CPh)_6(Im)_3]^+$.

better associated with transitions inherent in the bent diferric Fe–O–Fe unit rather than with the other bridging ligands. Consistent with this idea, these two bands have been assigned to ligand field transitions that gain intensity either by mixing with the intense near-UV oxo → Fe CT transitions or because of relaxation of the usual spin restrictions due to antiferromagnetic coupling.[55,62] The 480–510-nm band is assigned to a spin flip within the e_g orbitals, and, if so, its energy would be fairly independent of the ligand field.[59] A band at 477 nm in the spectrum of $enH_2[(FeHEDTA)_2O]\cdot 6H_2O$ has been assigned to this spin-flip transition.[60]

Resonance Raman excitation profiles of ν_s(Fe–O–Fe) in several tribridged complexes (cf. Figure 5) maximize at ~400 and ~530 nm, but these wavelengths do not correspond to prominent features in the absorption spectra.[55,63] These maxima in the Raman excitation profiles have been assigned to weakly allowed oxo → Fe CT transitions involving the d_{xy} orbitals in the bent Fe–O–Fe unit (represented as dotted vertical lines in Figure 4C).[59] These transitions are also π-derived, and according to the diagram of Figure 4, the energy separation between these two bands (~5500 cm^{-1} in Figure 5) is the difference in energy between the two oxygen π-type orbitals from which these transitions originate, as had been proposed earlier.[63]

V. IR and Raman Spectra

A. Vibrational Modes

Since the focus of this paper is on the Fe–O–Fe unit, vibrations external to this unit are not discussed. The vibrational analyses usually use an analogous simplifying assumption; i.e., the Fe–O–Fe linkage can be satisfactorily treated as an independent vibrational unit. The Fe–O–Fe unit has three vibrational modes: a symmetric Fe–O–Fe stretch (ν_s), an asymmetric Fe–O–Fe stretch (ν_{as}), and an Fe–O–Fe bending mode. Table II lists frequencies of the former two modes for the (μ-oxo)diiron(III) complexes, which are the only ones that have been analyzed in detail. In many cases the assignments in Table II have been verified by ^{18}O substitution into the bridge. Little data exist on vibrations of the M–O(H)–M unit for any metal. The μ-O–H stretch has been identified at 3560 cm^{-1} in the IR spectrum of the (μ-hydroxo)bis(μ-carboxylato)diiron(III) complex $[Fe_2(OH)(OAc)_2(HB(pz)_3)_2](ClO_4)\cdot 0.5CH_2Cl_2$.[51] The same stretch appears in the 3400–3500-cm^{-1} region for the bis(μ-hydroxo)diiron(III) complexes $[Fe(Chel)(H_2O)(OH)]_2\cdot 4H_2O$ and $[Fe(dipic)(H_2O)(OH)]_2$.[16] These latter complexes also show an IR band at ~900 cm^{-1}, which has been assigned to a $Fe(OH)_2Fe$ deformation mode. These deformation frequencies are included in Table II. The remaining discussion focuses on the (μ-oxo)diiron(III) complexes.

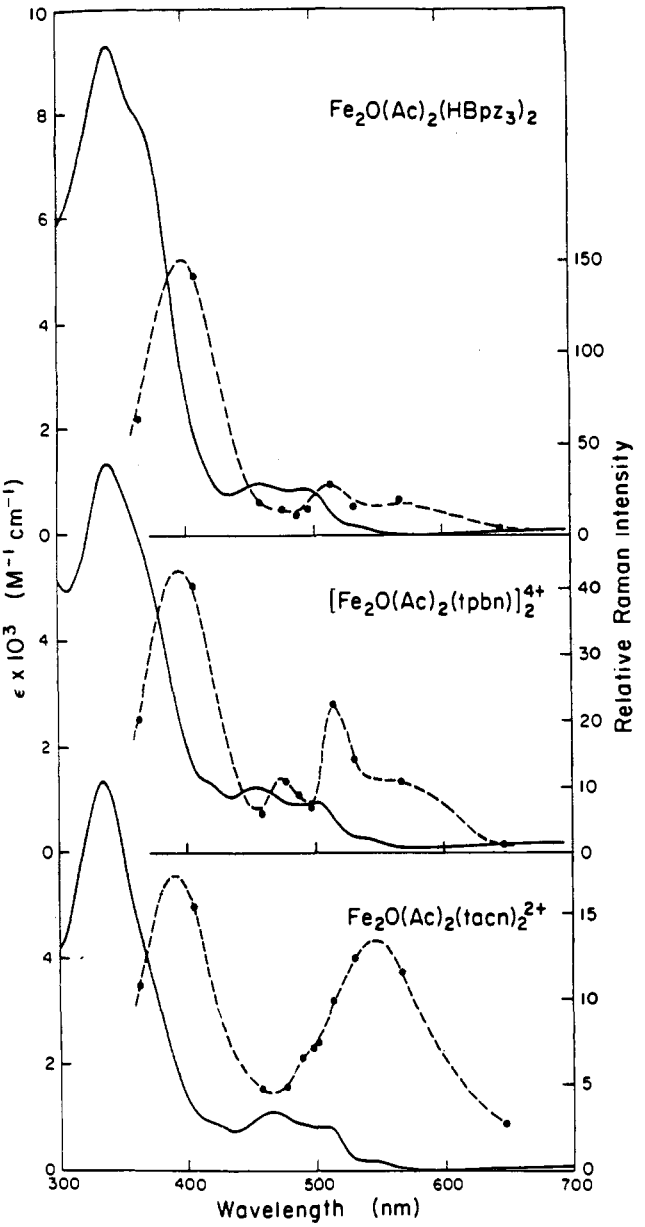

Figure 5. Electronic absorption spectra and Raman excitation profiles of ν_s(Fe–O–Fe) for $[Fe_2O(OAc)_2(HB(pz)_3]$, $\{[Fe_2O(OAc)_2(tpbn)_2]_2\}^{4+}$, and $[Fe_2O(OAc)_2(TACN)_2]^{2+}$ (reprinted from ref 55; copyright 1989 American Chemical Society).

B. (μ-Oxo)diiron(III) Complexes

In these complexes, the symmetric stretch of the Fe–O–Fe unit occurs between 380 and 540 cm^{-1} and the asymmetric stretch occurs between 725 and 885 cm^{-1}. Because of their point group symmetries, the former has the higher intensity in Raman spectra, while the latter is more readily observed in IR spectra. The first overtone of the asymmetric stretch is also Raman-active.[55] These frequencies have been analyzed[30,31,54,55] according to the equations of Wing and Callahan[64] for the two stretching modes of an M–O–M unit that have C_{2v} symmetry

$$A_1 \quad \lambda_s = [\mu_M + \mu_O(1 + \cos\phi)](k + k_{MOM}) \qquad (11)$$

$$B_2 \quad \lambda_{as} = [\mu_M + \mu_O(1 - \cos\phi)](k - k_{MOM}) \qquad (12)$$

where $\lambda = (5.889 \times 10^{-7})\nu^2$, ν being the frequency (cm^{-1}), k is the M–O stretching force constant and k_{MOM} is the stretch–stretch interaction constant (mdyn/Å), ϕ is the

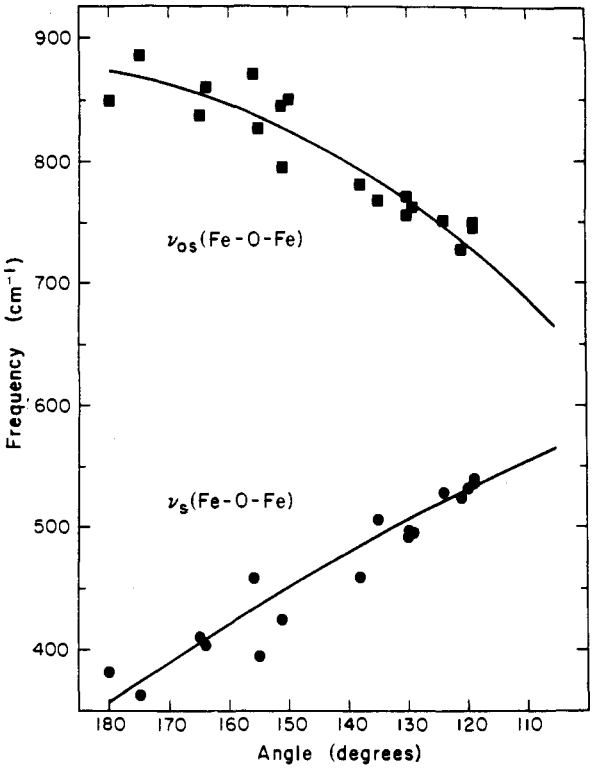

Figure 6. Correlation of the Fe–O–Fe symmetric and asymmetric stretching frequencies with observed Fe–O–Fe angle (reprinted from ref 55; copyright 1989 American Chemical Society).

M–O–M angle (deg), and μ_M and μ_O are the reciprocal masses of the labeled atoms. Figure 6 contains plots of ν_s and ν_{as} vs ϕ for several of the complexes listed in Table II.[55] A fairly smooth dependence is obtained over a wide range of angles, even though no discrimination is made between mono-, di-, and tribridged complexes in this plot. The data of Figure 6 indicate that Fe–O–Fe angles can be predicted within 10° from knowledge of ν_s and ν_{as}. Equations 11 and 12 predict linear relationships between the square of the frequency and cos ϕ, assuming that the force constants do not change. An empirical equation with this linear relation was found to fit the data well for the symmetric stretch; i.e., angles could be predicted within 6°.[54] The analogous linear relationship for the asymmetric stretch does not fit the data well. An accurate estimate of the Fe–O–Fe angle can also be made from eq 11 with the ^{16}O and ^{18}O symmetric stretching frequencies.[55] Normal-coordinate analyses using a general valence force field with the FG matrix method, and assuming an Fe–O–Fe bending frequency of 100 cm^{-1}, lead to $k \sim 3.3$ mdyn/Å and $k_{MOM} \sim 0.1$–0.6 mdyn/Å for the diferric complexes of Table II.[55,63] The value for the Fe–O–Fe bending frequency was confirmed by observation of an ^{18}O-sensitive band at 104 cm^{-1} in the Raman spectrum of $[Fe_2O(OAc)_2(HB(pz)_3)_2]$.[63]

Excitation profiles of the scattering intensity for the symmetric Fe–O–Fe stretching band in Raman spectra have assisted in assignment of electronic transitions in these complexes.[31,55,63] As shown in Figure 5, maximal resonance enhancement of this stretching band does not usually occur at the most prominent electronic absorption maxima of these complexes. The explanation often given for this observation is that resonance enhancement is most probable for those vibrational modes that mimic the excited-state geometry for a given

electronic transition. Excitation profiles of many compounds indicate that the intensity of the symmetric Fe–O–Fe stretching band is also elevated by multiple bridging groups and unsaturated terminal nitrogen ligands, especially those trans to the oxo bridge.[55] For example, $[Fe_2O(OPr)_2(tmip)_2](PF_6)_2$, which contains terminal imidazolyl ligands (cf. Figure 3), shows the highest relative Raman intensity of the symmetric Fe–O–Fe stretching band of all the synthetic compounds so far examined.[55] The unsaturated nitrogen ligands may facilitate delocalization of π-electron density within the Fe–O–Fe unit. This explanation assumes that π-derived oxo → Fe CT transitions are the source of resonance enhancement for the symmetric Fe–O–Fe stretch. The maximal Raman scattering intensity of the symmetric Fe–O–Fe stretch is reported to be about the same for $[Fe_2O(OAc)_2\{[OP(OEt)_2]_3Co(C_5H_5)\}_2]$, which has terminal phosphate-type oxygen ligands to iron, as for $[Fe_2O(OAc)_2(HB(pz)_3)_2]$, which has terminal pyrazolyl nitrogen ligands.[33] Therefore, this effect on Raman scattering intensity is apparently not confined to unsaturated nitrogen ligands.

VI. Magnetism

A. Antiferromagnetism

Spin–spin coupling in diiron complexes is usually well-approximated by the general isotropic spin-exchange Hamiltonian, $\hat{H}_{ex} = -2JS_1 \cdot S_2$.[65] The eigenvalues are simply determined from vector coupling of all unpaired spins on the two iron atoms, and the magnitude of J signifies the strength of interaction between the spins. $-J$ values using the $2J$ formalism are listed in Table II, together with room-temperature effective magnetic moments. Sets of values for a few additional compounds may be found in the earlier review.[1] The sign convention used throughout this paper is that negative values of J signify antiferromagnetic coupling, i.e., where the ground state has minimum spin multiplicity. (The reader is warned that this sign convention and the $2J$ formalism are not universally used in the literature.) Earnshaw and Lewis were the first to suggest antiferromagnetic coupling as an explanation for the magnetic behavior for oxo-bridged diiron(III) complexes,[66] and this explanation remains widely applicable. In fact, where such measurements have been made, the oxo-bridged and all but one of the hydroxo-bridged synthetic diiron complexes invariably show temperature-dependent variations in magnetic susceptibility indicative of antiferromagnetism. The temperature dependences are due to Boltzmann-weighted populations of the various spin states that result from antiferromagnetic coupling. The ladders of spin states for the three oxidation levels of the oxo/hydroxo-bridged diiron complexes most commonly encountered in chemistry and biology are shown in Figure 7. Susceptibility vs temperature curves for several values of J and equations for calculating these curves in the three cases of Figure 7 have been published.[67,68] The diferric case was discussed explicitly by Murray.[1] Therefore, no detailed discussion is given here. $-J$ values for the vast majority of oxo-bridged diiron(III) complexes fall into the 80–120-cm^{-1} range. The porphyrin-ligated species tend to have slightly higher values (120–140 cm^{-1}), perhaps reflecting their nearly linear geometry

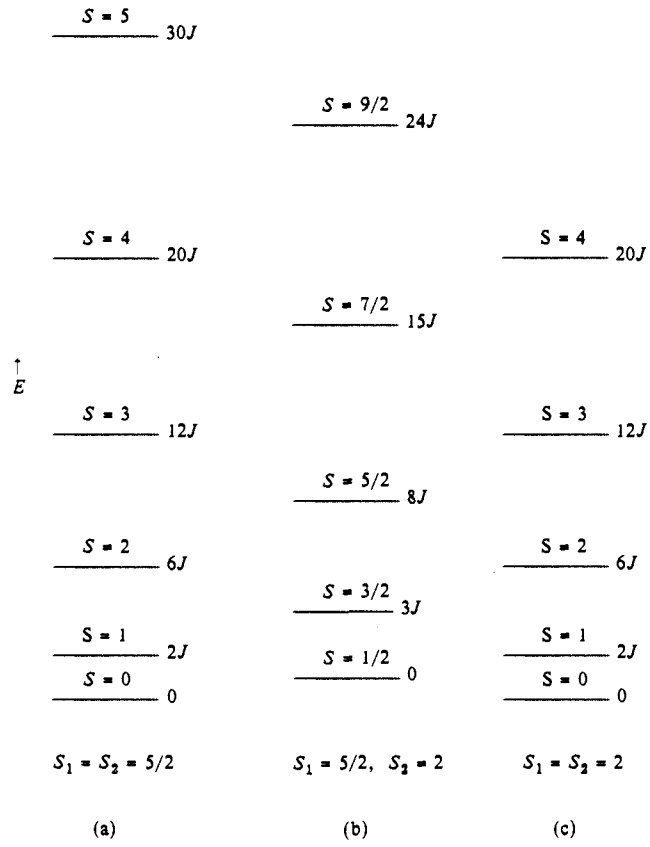

Figure 7. Energy levels of the spin states resulting from antiferromagnetic coupling of spins on $Fe^{III}Fe^{III}$ (a), $Fe^{II}Fe^{III}$ (b), and $Fe^{II}Fe^{II}$ (c). The relative energies of each level are listed as multiples of J, the antiferromagnetic coupling constant in the Hamiltonian for isotropic exchange, $\hat{H} = -2JS_1 \cdot S_2$. Since the magnitude of J will in general be unequal for a–c, the energy scale will be different for the three cases.

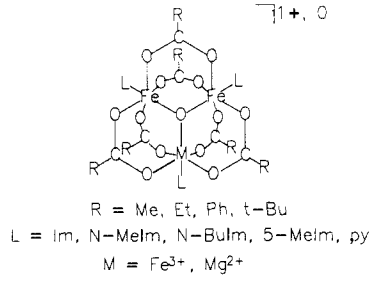

Figure 8. "Basic iron acetate" schematic structure and examples of substituents (cf. refs 34 and 69).

and slightly shorter Fe–O(oxo) bond lengths (Tables I and II). The lower value of $-J$ (62 cm^{-1}) for $[Fe_2MgO(OAc)_6(py)_3]$[69] is presumably due to the Mg–O(oxo) bond in the "basic iron acetate" structure of this complex, as illustrated in Figure 8. The (μ-hydroxo)diiron(III) complexes have $-J$ values in the 7–17-cm^{-1} range, with the bis(μ-hydroxo) complexes being at the lower end of this range.

B. Methods for Measurement of $-J$

For comparison purposes a few comments concerning uncertainties in the J values of Table II are perhaps warranted. These values have almost invariably been determined from fits of magnetic susceptibility (or a related function) vs temperature curves to the equations referred to above. Due to variability in the way these fits are obtained (e.g., inclusions of corrections for

diamagnetism of the ligands, temperature-independent paramagnetism, and paramagnetic impurities and allowing g to vary from the free electron value), differences in J values of up to 10% may not be significant when they originate from different laboratories. An additional complication for weakly coupled mixed-valent and diferrous systems is that the axial zero-field splitting energy D can be comparable to J. In such cases inclusion of D can significantly perturb the energies and, hence, the populations of spin levels with $S \geq 1$. Here again, D is usually estimated and/or allowed to vary in the fitting procedure, and in these cases the solutions obtained are not necessarily unique.

The data in Tables II and III show that the room-temperature effective magnetic moment provides a reliable estimate of the magnitude of J for the diferric complexes. The moments listed in Table II are those measured on solids, whereas those listed in Table III were measured in solution by the Evans NMR method.[34,35] Where comparisons have been made on the same compounds,[27,30,35,51,54] the magnetic moments measured on solids are in excellent agreement with those obtained in solution. Such comparisons demonstrate the utility of the Evans method for ascertaining the integrity of the complex in solution.

J values for most synthetic oxo/hydroxo-bridged species have been determined by measurements of magnetic susceptibility vs temperature on a Faraday balance or SQUID susceptometer. Because these methods are more difficult to apply to iron centers in proteins, indirect methods for estimating J have been developed. These include temperature and field dependences of MCD intensities,[58] temperature dependences of Orbach EPR relaxation,[70] and NMR isotropic shifts. The last method is discussed below.

The most recent studies of ^{1}H NMR chemical shifts of bridging acetate methyl groups and terminal imidazoles in tribridged high-spin diferric complexes indicate a monotonic (but nonlinear) correlation between $-J$ and μ_{eff}^2/Fe (cf. Table III).[34] Note that the "basic iron acetate" structure of $[Fe_3O(OAc)_6(Im)_3]^+$ (illustrated schematically in Figure 8) contains dinuclear tribridged fragments that are identical with those of the other tribridged μ-oxo/hydroxo complexes listed in Table III, and pairwise $-J$ values for this trinuclear complex are available.[71] An approximate correlation of these $-J$ values with chemical shift is apparent, and these shifts can, therefore, be used to set limits on $-J$ for structurally similar complexes. For weakly coupled systems $-J$ can also be estimated from the temperature dependence of ligand isotropic shifts. The method consists of fitting the slope of the isotropic shift vs temperature curve to the susceptibility expected over the same temperature range. In the range accessible to most solution NMR experiments (~0–60 °C for proteins) this slope will be small (or zero at the Neel temperature) for $-J \gtrsim 30$ cm^{-1}. This statement applies to both the diferric and mixed-valent systems. The small temperature variation of isotropic shifts for more strongly coupled systems tends to make such determinations error prone. Also, for more strongly coupled systems, the populations of the various spin levels of the manifold may change significantly over the accessible temperature range according to a Boltzmann distribution. If these levels have different electron–nuclear hyperfine coupling constants, then the isotropic shifts (even if exclusively contact in origin) will not be linearly related to magnetic susceptibility. This point was discussed in Murray's review.[1] Dipolar contributions to the isotropic shifts also make this method unreliable for diferrous complexes. For the mixed-valent iron sites of hemerythrin and uteroferrin, $-J$ values of 10–30 cm^{-1} have been determined from the temperature dependence of isotropic shifts of ligands to the *ferric* center.[72,73] These values were later verified by other means.[69,74]

$-J$ values of ~140–150 cm^{-1} have been determined from the temperature dependence of ^{13}C NMR isotropic shifts of the pyrrole carbons in synthetic diferric oxo-bridged porphyrin complexes.[75,76] The larger dispersion of ^{13}C signals means that reasonable variations with temperature can be obtained even for such strongly coupled systems. The temperature variation was fit by use of different hyperfine coupling constants for the $S = 1$ and 2 spin levels. For $-J$ values of 140–150 cm^{-1}, these excited spin levels are the only ones significantly populated near ambient temperature. These $-J$ values are in reasonably good agreement with those determined from measurements on analogous solids.[75,77-79]

C. Other Types of Spin Coupling

No Heisenberg ferromagnetic oxo/hydroxo-bridged diiron molecular species has yet been synthesized. Ferromagnetic coupling in the azide and cyanate adducts of deoxyhemerythrin has been observed and analyzed by MCD spectroscopy; the ground state is concluded to be $S = 4$.[58] Protonation of the hydroxo bridge to form an aqua bridge upon formation of the adducts has been proposed to account for the switchover from antiferromagnetism. Synthetic aqua-bridged diiron complexes remain an unrealized goal.

Very recently a novel type of spin coupling has been described for the mixed-valent complex $[Fe_2(MTACN)_2(\mu\text{-}OH)_3]^{2+}$, which has the tris($\mu$-hydroxo) structure (cf. Figure 1).[26] This complex is valence-delocalized (i.e., class III in the Robin–Day scheme)[80] and is Heisenberg antiferromagnetic but shows an $S = {}^9/_2$ ground state due to so-called double exchange. For such valence-delocalized systems the ground spin state will depend on the relative magnitude of $-J$, which favors the lowest spin multiplicity, vs that of the electron-transfer integral B, which favors the highest spin multiplicity. (For an excellent discussion of and leading references to the phenomenon of double exchange cf. ref 81.) For the high-spin $Fe^{II}Fe^{III}$ system, double exchange dominates when $|B/J| \geq 4.5$. Of course, for valence-localized systems, $B = 0$ and the system will be either antiferromagnetic or ferromagnetic, depending on the sign of J. Examples of both of the latter types exist for phenoxo-bridged $Fe^{II}Fe^{III}$ complexes.[82] The spin state ladder for $S = {}^9/_2$ ground-state systems is in the reverse order of that shown in Figure 7b.

D. Orbital Pathways for Spin-Exchange Coupling

The preceding analyses of magnetic behavior have been based solely on solutions to phenomenological Hamiltonians for the various possible interactions of electron spins. These analyses are useful because they fit the observed behavior well in most cases and because the magnitude of $-J$ can be used to identify the bridging

ligands. This latter usefulness is illustrated in the cases of methemerythrin (μ-oxo) and deoxyhemerythrin (μ-hydroxo), whose bridging ligands were confirmed by comparisons of their $-J$ values to appropriate synthetic models.[3,4,52,58] The overwhelmingly favorable route for transmission of the spin–spin interactions is through orbitals on each iron atom and those on the bridging ligands. Therefore, the magnitude and sign of J must be related to the bonding in these complexes. π bonding across the bridge is often invoked as the major pathway for antiferromagnetic coupling. However, the orbitals involved in spin-exchange coupling in diiron complexes have not been conclusively identified. One problem is the large number of orbital pathways for spin exchange, both ferromagnetic and antiferromagnetic, that are possible in these systems. These pathways, some of which are implied in the diagrams of Figure 4, were enumerated explicitly many years ago by Ginsberg.[83] Another problem is that the dominant pathways may depend on structural parameters, such as the Fe–O–Fe angle. A few relevant trends have emerged for the diferric systems, however. The similarity in J values for a large number of μ-oxo mono-, di-, and tribridged complexes (Table II) shows that antiferromagnetic pathways dominate over ferromagnetic pathways and that in multibridged complexes the oxo bridge is the dominant mediator of spin-exchange coupling. A hydroxo bridge mediates a much smaller degree of antiferromagnetic coupling than does an oxo bridge. In the μ-oxo-monobridged structural subcategory, decreasing the Fe–O–Fe bridge angle from 180° causes a small but significant decrease in the strength of antiferromagnetic coupling. The relevant comparisons (for which measurements were made in the same laboratories) are $[Fe(salen)]_2O$ (Fe–O–Fe = 145°, $-J$ = 92 cm^{-1}) vs $[Fe(3\text{-}t\text{Busaltmen})]_2O$ (Fe–O–Fe = 173°, $-J$ = 100 cm^{-1})[27] and two crystalline forms of $[Fe(Pc)]_2O$ (linear Fe–OFe, $-J$ = 195 cm^{-1}, vs nonlinear Fe–O–Fe, $-J$ = 120 cm^{-1}).[84,85] An empirical equation that relates $-J$ values to an inverse exponential of Fe–O(oxo) distances has been shown to be valid for a large number of diferric compounds and larger iron–oxo aggregates containing two or more bridging ligands.[54,86] If nothing else, these structural correlations illustrate the sensitivity of antiferromagnetic coupling strength to overlaps between half-filled d orbitals on the iron atoms and the filled orbitals on the oxo bridge. Kahn and Briat[87] and Hay et al.[28] have separately analyzed antiferromagnetic coupling in dinuclear systems from a molecular orbital viewpoint. The analyses assume that antiferromagnetic coupling can be treated essentially as incipient bond formation involving those d orbitals that contain unpaired electrons (often referred to as the magnetic orbitals) with contributions from the bridge atom orbitals. In both cases the equations resulting from these analyses are of the form

$$J = (1/n^2)\sum J_{ij} \qquad (13)$$

where J is the antiferromagnetic exchange coupling constant, n is the number of unpaired electrons on each metal atom (which is equal to the number of magnetic orbitals), and J_{ij} are functions of overlap integrals between magnetic orbitals on each metal atom mediated by the bridging ligand and of the energy separations between the symmetric and antisymmetric combinations of these orbitals. The sum is over all magnetic molecular orbitals. Overlap considerations suggest that only a few J_{ij} have large values, i.e., that a few exchange pathways dominate.[27,29,87] Extended Hückel calculations have been done on the diferric μ-oxo-monobridged systems with a linear or nearly linear Fe–O–Fe unit.[27,29] These calculations indicate that the decrease in $-J$ with decrease in Fe–O–Fe angle is due mainly to a decrease in the energy separation between the magnetic molecular orbitals, $\phi_S = (d_{xz} + p_x - d_{xz})$, and $\phi_A = (d_{xz} + d_{xz})$:

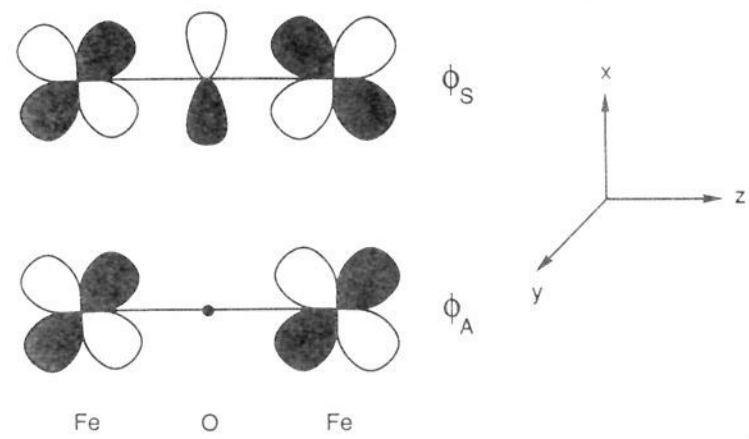

These orbitals imply a π superexchange pathway. For nonlinearity the above molecular orbitals are useful approximations. The composition of ϕ_A and ϕ_S can change upon departure of the Fe–O–Fe angle from 180° due to symmetry lowering and changes in orbital overlaps. ϕ_A, for example, becomes considerably mixed with d_{z^2} upon bending and is destabilized relative to ϕ_S.[27]

If a few superexchange pathways dominate for a given structural type (e.g., a fixed Fe–O–Fe angle), then eq 13 implies that the strength of antiferromagnetic coupling should be roughly inversely proportional to the square of the number of unpaired electrons. The published J values for the sets of (μ-oxo)bis(μ-carboxylato)dimanganese(III) vs -diiron(III) congeners $[Mn_2O(OAc)_2(HB(pz)_3)_2]$ (~ -0.5 cm^{-1})[88] vs $[Fe_2O(OAc)_2(HB(pz)_3)_2]$ (-121 cm^{-1}),[30] $[Mn_2O(OAc)_2(MTACN)_2](ClO_4)_2$ ($+9$ cm^{-1})[89] vs $[Fe_2O(OAc)_2(MTACN)_2](ClO_4)_2 \cdot H_2O$ (-129 cm^{-1}),[32] and $[Fe_2O(OAc)_2(tmip)_2](ClO_4)_2 \cdot CH_3CN$ (-120 cm^{-1}) vs $[Mn_2O(OAc)_2(tmip)_2](PF_6)_2$ ($\lesssim 0.5$ cm^{-1})[35] represent a clear case of *disagreement* with the calculated ratio of J values (25/16), assuming that the same exchange pathways are dominant. The structural parameters of the Mn and Fe congeners, including the M–O(oxo) distances and M–O–M angles, are quite similar to each other. Clearly the dominant magnetic orbitals must be different in these tribridged diiron(III) and dimanganese(III) complexes. The pattern of trans vs cis Mn–N distances and of ^1H NMR isotropic shifts for $[Mn_2O(OAc)_2(HB(pz)_3)_2]$[88] and $[Mn_2O(OAc)_2(tmip)_2](PF_6)_2$[35] shows that the d_{z^2} orbitals (i.e., those that are directed along the M–O(oxo) axis) are empty in the dimanganese(III) complexes, whereas these orbitals must be half-occupied in the diiron(III) complexes. This comparison suggests a potentially useful approach to identification of the dominant magnetic orbitals in (μ-oxo)dimetal(III) complexes. Bossek et al.[175] present an elegant demonstration of this approach, which suggests that the d_{z^2}–d_{xz} "crossed" pathway is important when the M–O–M angle is $\sim 120°$.

The single apparent example of a low-spin diferric Fe–O–Fe system, namely the set of $[(N\text{-base})PcFe]_2O$ complexes, has a relatively modest antiferromagnetic

coupling ($-J \sim 6$ cm^{-1}) of the two $S = {}^1/_2$ centers.[90] The crystal structure of the complex where N-base = *N*-MeIm indicates an oxo bridge with a nearly linear Fe–O–Fe angle.

E. Oxidation Levels Other than Diferric

The small number of lower valent complexes precludes any detailed analyses of exchange coupling in these systems. The single example of a diferrous complex, $[Fe^{II}_2(\mu\text{-}OH)(OAc)_2(MTACN)_2](ClO_4)\cdot H_2O$, has $-J$ = 13 cm^{-1},[32,52] which is presumably mediated almost entirely through the hydroxo bridge. A comparison with the $-J$ value for the manganese congener $[Mn^{II}_2(\mu\text{-}OH)(OAc)_2(MTACN)_2](ClO_4)$ (9 cm^{-1})[89] shows quite good agreement with the calculated ratio of $-J$ values (25/16) from eq 13. Quantitative comparison with $-J$ of the hydroxo-bridged diiron(III) complex $[Fe_2(OH)(OAc)_2(HB(pz)_3)_2](ClO_4)\cdot 0.5CH_2Cl_2$ ($-J$ = 17 cm^{-1})[51] using eq 13 is probably not warranted because of the different capping ligands, distances, and angles in the diferric vs diferrous complexes.

The magnitude of spin-exchange coupling for mixed-valent oxo- or hydroxo-bridged systems has not been established. Temperature-dependent magnetic data are unavailable for the single structurally characterized oxo-bridged mixed-valent complex $\{Na[Fe^{II,III}(acen)]_2O\}_2$;[24] such measurements are awaited with great interest. The single structurally characterized example of a hydroxo-bridged mixed-valent diiron system is $\{[Fe(MTACN)]_2(\mu\text{-}OH)_3\}(ClO_4)_2\cdot 2CH_3OH\cdot 2H_2O$.[26] However, extrapolation to other cases is complicated by the $S = {}^9/_2$ ground state of this complex due to double exchange as discussed above and by its unusually short Fe–Fe distance (~2.5 Å). The mixed-valent oxidation level of the diiron site in hemerythrin has $-J$ = 15–20 cm^{-1},[70,72] which is sometimes cited as evidence for a hydroxo bridge, based on the expectation that an oxo bridge would mediate much stronger coupling. This expectation is apparently based on extrapolation from the diferric systems. If all other factors remain unchanged, one would indeed expect a hydroxo bridge to mediate weaker coupling than an oxo bridge, due to withdrawal of electron density by the proton.[28] However, predictions about the magnitude of $-J$ in an oxo-bridged mixed-valent system based on that of the oxo-bridged diferric system are risky due to possible Fe–O(oxo) bond lengthening[24,25] and changes in the nature and energies of the dominant magnetic orbitals upon conversion to a mixed-valent species.

$-J$ values for a few $Fe^{III,IV}$ mixed-valent diiron species resulting from oxidations of $[Fe(salen)]_2O$ and $[Fe(TPP)]_2O$ have been reported in the range of 8–17 cm^{-1},[91] but the nature of the bridging group(s) in the oxidized forms is uncertain.

VII. EPR Spectra

A. Half-Integer Spin Ground States

Of the three cases shown in Figure 7, the half-integer spin systems resulting from magnetic coupling at the $Fe^{II}Fe^{III}$ oxidation level (Figure 7b) are expected to elicit the most readily observable EPR signals. Indeed, characteristic $S = {}^1/_2$ EPR signals with average g values less than 2 are observed below ~30 K for the mixed-valent oxidation level of diiron sites in proteins such as hemerythrin and the hydroxylase of methane monooxygenase.[70,92] An EPR signal centered at g = 1.95 was obtained at 77 K upon reductive electrolysis of $[Fe(TTP)]_2O$[93] and was attributed to the oxo-bridged $Fe^{II}Fe^{III}$ species. This mixed-valent species was not isolated or otherwise characterized. Similarly, a species prepared in situ by electrochemical reduction of a solution of $[Fe_2O(OAc)_2(MTACN)_2](PF_6)_2$ shows an EPR spectrum at 10 K with g values of 1.95 and 1.89,[32] which are similar to those of mixed-valent diiron sites in proteins. Here again, this species has not been isolated in pure form. The only other reported EPR for a synthetic oxo/hydroxo-bridged mixed-valent diiron species arises from the $S = {}^9/_2$ ground state of $\{[Fe_2(MTACN)]_2(\mu\text{-}OH)_3\}(ClO_4)_2\cdot 2CH_3OH\cdot 2H_2O$, which shows features at $g \sim 10$ and 2–2.5.[26] The specific transitions giving rise to these features have yet to be identified.

B. Integer Spin States

A few reports of EPR signals arising from oxo-bridged diferric species were included in Murray's earlier review.[1] These reports were all of a preliminary nature, and none of them have apparently been pursued. A similar pattern has occurred during the intervening years. A few further reports of EPR signals from oxo- and hydroxo-bridged diferric complexes either are preliminary analyses[94-96] or are of the "fingerprint" type. These spectra are usually of powdered solids at either 77 K or room temperature.[51,85,97-99] There appears to be no discernible pattern to these spectra among the various reports, with signals appearing anywhere from 500 to 6000 g at X-band. The preliminary analyses attribute some of these signals to the S = 1 and 2 excited states illustrated in Figure 7a. The magnitude of $-J$ for the oxo-bridged species dictate that only these states would be appreciably populated up to ambient temperature. While non-Kramers systems are normally difficult to observe by EPR, several recent reports show that, under favorable conditions, EPR signals arising from S = 2 and 4 states of iron complexes are observable, and from analyses of these spectra the signals can be attributed to specific transitions within these states.[100] These signals have invariably arisen from ground spin states and are observable only at low temperatures. A pertinent example is the azide adduct of the diferrous site in deoxyhemerythrin, which, as mentioned above, is ferromagnetic. Below 40 K this adduct shows a broad EPR transition at <1000 G ($g_{eff} \sim 13$), which has been ascribed to the $M_S \pm 4$ transition within the S = 4 ground state.[58,100b] A very similar signal has recently been reported for the diferrous site in methane monooxygenase.[92] The problem in the oxo-bridged diferric system is that because the paramagnetic spin states are excited states, temperatures that significantly populate these states are likely to cause rapid relaxation of the electron spin, making observations of EPR signals extremely difficult. The weakly coupled hydroxo-bridged diferric systems would require lower temperatures to populate the upper states and may offer the best chance for observation of integer spin EPR signals. Whether or not such signals are observable also depends critically on the magnitudes and signs of the zero-field splittings. At this juncture

EPR cannot be considered a reliable probe of antiferromagnetically coupled integer-spin diiron complexes.

VIII. Mössbauer Spectra

For diiron complexes Mössbauer spectroscopy has proven to be the most efficient method for establishing (i) oxidation and spin states of the iron atoms, (ii) diamagnetism and paramagnetism of the ground state for diferric and mixed-valent oxidation levels, respectively, and (iii) valence localization/delocalization in the solid state for mixed-valent complexes. Isomer shifts (δ_{Fe}) and quadrupole splittings (ΔE_Q) are listed in Table II. Data for a dozen additional compounds are tabulated in Murray's earlier review.[1] Isomer shifts in the range 0.35–0.60 mm/s are characteristic of 5- or 6-coordinate high-spin diferric μ-oxo and μ-hydroxo complexes. The $[Fe_2OCl_6]^{2-}$ salts have lower isomer shifts ($\sim$0.22 mm/s), as is usual for tetrahedral high-spin ferric ion. The majority of the oxo-bridged diferric complexes have quadrupole splittings >1 mm/s, the porphyrin and phthalocyanine complexes being notable exceptions. All of the hydroxo-bridged diferric complexes have quadrupole splittings <1 mm/s, as do most mononuclear high-spin ferric complexes.

A useful comparison can be made for the (μ-oxo)bis(μ-carboxylato)diiron(III) complexes $[Fe_2O(OAc)_2(HB(pz)_3)_2]$ and $[Fe_2O(OPr)_2(tmip)_2]^{2+}$ vs their μ-hydroxo counterparts $[Fe_2(OH)(OAc)_2(HB(pz)_3)_2]^+$ and $[Fe_2(OH)(OPr)_2(tmip)_2]^{3+}$. The isomer shifts of all four complexes are similar to each other (0.45–0.52 mm/s), whereas the quadrupole splittings are 1.27–1.80 mm/s for the oxo-bridged and 0.25–0.56 mm/s for the hydroxo-bridged complexes. The reduction in electric field gradient indicated by the smaller quadrupole splittings in the hydroxo-bridged complexes may be due to lengthening of the Fe–O(oxo) bond upon protonation of the oxo bridge. Thus, in these tribridged diferric complexes a quadrupole splitting of $\sim$1.6 mm/s appears to be characteristic of a short ($\sim$1.8-Å) Fe–O distance, whereas a significantly smaller quadrupole splitting indicates a lengthening of this bond. The data of Table II indicate a similar pattern for the dibridged μ-oxo vs μ-hydroxo complexes, although a direct comparison cannot yet be made. It should be emphasized that quadrupole splittings will also be sensitive to other changes in the coordination sphere.

The diamagnetism of the ground spin state in the diferric complexes can be confirmed by lack of broadening or splitting of the quadrupole doublet at 4 K in an external magnetic field of $\lesssim$2000 G. Conversely, the paramagnetic ground states of mixed-valent complexes are manifested as a broadening or splitting in an externally applied magnetic field at 4 K.[26]

IX. Reactivity

As mentioned in the Introduction, reports on reactivity of the title complexes are limited. One reason for this limitation must be the stability of the diferric Fe–O–Fe unit, which translates to inertness. A second reason is instability of the mixed-valent and diferrous units, which (so far) translates to a lack of selectivity. Protonation and bridge exchange/substitution reactions were discussed in Synthesis; reactions leading to higher nuclearity are discussed elsewhere.[5] Aside from these, the reported reactivities of the title complexes are mainly redox in nature. The single example of chemical reduction of an oxo-bridged diferric complex resulting in a structurally characterized mixed-valent complex[24] was discussed in Synthesis.

A. Electrochemistry

Cyclic voltammetry of $[Fe(salen)]_2O$, and $[Fe(TPP)]_2O$ show chemically reversible one-electron reductions at $E_{1/2} \sim -1$ V vs SCE.[28,93,101] Subsequent reduction steps are irreversible. The tribridged complex $[Fe_2O(OAc)_2(MTACN)_2]^{2+}$ also shows a quasi-reversible one-electron wave at $E_{1/2} \sim -0.37$ V vs SCE.[31] For these three complexes, controlled-potential coulometry results in production of metastable mixed-valent species, which have resisted all attempts at isolation. A quasi-reversible reduction process, which was assumed to involve the mixed-valent form, has been reported for the unsymmetrical μ-oxo-monobridged complex $[Fe_2O(N5)Cl_3]Cl$.[20] In contrast to the behavior of $[Fe_2O(OAc)_2(MTACN)_2]^{2+}$, the tribridged complexes with $HB(pz)_3$ as capping ligand exhibit only irreversible electrochemical reduction waves, with formation of $[Fe(HB(pz)_3)]^+$.[30,54] As discussed in Synthesis, MTACN for steric reasons tends not to form the analogous bis-complex so readily. $[Fe_2O(OAc)_2\{[OP(OEt)_2]_3Co(C_5H_5)\}_2]$, whose tribridged core is capped by the tripodal oxygen-donor ligand $\{[OP(OEt)_2]_3Co(C_5H_5)\}^-$, also displays a quasi-reversible reduction wave and shows no evidence for formation of $[Fe\{[OP(OEt)_2]_3Co(C_5H_5)\}_2]^+$.[33] The nature of the reduced species is not yet known. One-electron electrochemical oxidations are chemically reversible for $[Fe(Pc)]_2O$[102] and $[Fe(TPP)]_2O$.[103a] In the case of $[Fe(TPP)]_2O$, a second oxidation wave is also reversible and both oxidations appear to be porphyrin- rather than iron-centered. The products of these oxidations have not been structurally characterized, but some spectroscopic and magnetic data are available.[102b,103a]

B. Oxygen Transfer and O_2 Activation

The few reactions involving transfer of the bridging oxygen are limited to $[Fe(TPP)]_2O$[47] and $[Fe(Pc)]_2O$.[103b] These reactions are throught to proceed by heterolytic cleavage of the Fe–O–Fe unit, with the resulting oxoferryl species being the oxygen-transfer agent. The TPP and Pc rings apparently favor production of this species. Triphenylphosphine is usually the acceptor. The photodisproportionation and oxygen atom transfer reactions 14 and 15 for $[Fe(TPP)]_2O$ and related por-

$$[Fe(TPP)]_2O \xrightarrow{h\nu} FeO(TPP) + FeTPP \quad (14)$$

$$FeO(TPP) + PPh_3 \rightarrow FeTPP + OPPh_3 \quad (15)$$

phyrin dimers are illustrative.[104] Oxidations of amines and olefins by (presumably) analogous photochemical reactions have also been reported. The quantum yields for reactions 14 and 15 increase with decreasing wavelength from 440 to 350 nm, arguing against involvement of the Soret transition of the porphyrin in the photochemistry. Charge-transfer excited states of the diferric Fe–O–Fe unit were instead invoked.[104b] A transition at 320 nm was noted for $[Fe(TPP)]_2O$. This wavelength is near the "oxo dimer" maxima of many oxo-bridged

diferric complexes (Table II). As discussed elsewhere in this review, these maxima have been assigned to oxo → Fe CT transitions.

Electrocatalytic oxidations of alkenes in the presence of $[Fe(TPP)]_2O$ and F^- are also thought to involve oxoferryl species.[102c] Oxygen transfer from *p*-cyano-*N*,*N*-dimethylaniline *N*-oxide to $[Fe(TPP)]_2O$ is reported to generate hypervalent iron–oxo species.[105]

A few laboratories have reported catalysis of oxygen insertion into organic substrates by μ-oxo mono- and tribridged diferric complexes.[36,106–108] Sources of oxygen include O_2, *t*-BuOOH, or "activated" O_2, produced by reduction over Zn powder in glacial acetic acid. Cyclohexane and adamantane are typical substrates, with the corresponding alcohols and ketones being the most abundant products. While turnover has been demonstrated in all of these systems, in no case has the active catalyst been established to be an oxo/hydroxo-bridged species. In one system the active catalyst is almost certainly *not* such a species.[106b] The mechanistic information, especially regarding involvement of iron, is sketchy in all cases and is, therefore, not summarized here. O_2 activation by iron is often associated with oxidation states higher than ferric,[47] but there is no clear synthetic precedent for involvement of polynuclear oxo/hydroxo-bridged iron complexes in O_2 activation. On the other hand, the obvious connection to methane monooxygenase makes this chemistry worth continued exploration. A pertinent reaction in this regard is the aerial oxidation of $[Fe^{II}_2(O_2CH)_4(BIPhMe)_2]$ in $CHCl_3$, which yields $[Fe_2O(O_2CH)_4(BIPhMe)_2]\cdot H_2O$. Oxygen from labeled O_2 was found to be incorporated into the oxo bridge of the product.[173]

X. Some Implications for Diiron Sites in Chemistry and Biology

As mentioned at the outset, much of the recent chemistry discussed in this review has been stimulated by biological considerations. It, therefore, seems appropriate to conclude with some insight into biological diiron sites provided by the synthetic models and vice versa.

A. "Spontaneous Self-Assembly" of the (μ-Oxo)diiron(III) Unit

Nature has apparently taken advantage of the spontaneous self-assembly of the (μ-oxo)bis(μ-carboxylato)diiron(III) core, since this core is found in methemerythrin.[109] The same statement may also apply to the dibridged (μ-oxo)(μ-carboxylato) core, although no protein as yet has been definitively shown to contain such a site. [See Note Added in Proof.] The (μ-oxo)(μ-carboxylato) complex $[Fe_2O(OBz)(hdp)_2]BPh_4$,[38] which contains terminal phenoxo and pyridyl ligands, may reflect the structure of the diiron site in purple acid phosphatases. There is currently no evidence for a μ-oxo-monobridged diiron complex at the active site of a protein. Heme proteins have been designed to isolate their iron–porphyrin prosthetic groups, thereby preventing reactions 3–7 that would lead to μ-oxo species. The lower stabilities of the synthetic mixed-valent and differous complexes do not rule out assemblies of such reduced sites within proteins. Little information is available regarding the oxidation state(s) of iron during assemblies of non-heme, non-sulfur diiron sites in vivo.

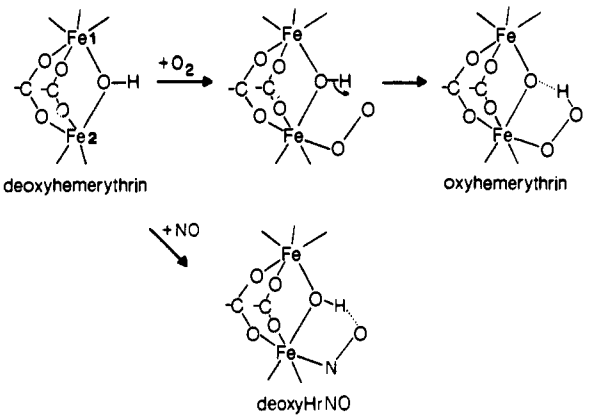

Figure 9. Proposed mechanism for reversible oxygenation of hemerythrin (reprinted from ref 110; copyright 1985 National Academy of Sciences) and proposed structure for the iron site of the nitric oxide adduct of deoxyhemerythrin (deoxyHrNO) (reprinted from ref 115; copyright 1987 American Chemical Society).

B. Structural Comparisons with the Diiron Site of Hemerythrin

1. Diferric and Diferrous Forms

The iron site structures of met- and azidomethemerythrin were known[109c] prior to those of the (μ-oxo)bis(μ-carboxylato)diiron synthetic models.[3,4] However, the synthetic models have greatly clarified important details of the iron site structures in the diferric and diferrous oxidation levels of hemerythrin.[5,30] For the synthetic tribridged complexes, the stable diferrous structure appears to require a hydroxo bridge,[32,52] whereas both μ-oxo and μ-hydroxo diferric species are known.[34,35,51] The structure and magnetic properties of the (μ-hydroxo)bis(μ-carboxylato)diiron(II) complex $[Fe_2(\mu\text{-}OH)(OAc)_2(MTACN)]^+$ [32,52] must closely resemble those of deoxyhemerythrin,[58] except that one of the iron atoms in deoxyhemerythrin has an open or labile coordination site for binding of O_2 according to reaction 16. The hydroperoxide in oxyhemerythrin is bound end-on to one iron atom and is hydrogen-bonded to the oxo bridge as shown in Figure 9.[110] The (μ-oxo)bis(μ-carboxylato)diiron(III) synthetic models, such as that depicted in Figure 3, can be considered structural analogues of the diferric site in azidomethemerythrin.[109] ^1H NMR isotropic shifts listed in Table III for the synthetic tribridged complexes, when compared to the analogous resonances of the proteins,[72] clearly demonstrate that a (μ-oxo)- rather than (μ-hydroxo)diferric complex is the best description of the iron sites in both met- and oxyhemerythrin. That is, in the product of reaction 16, the proton belongs on the peroxo ligand

$$\underset{\text{deoxy}}{[Fe^{II}(\mu\text{-}OH)Fe^{II}]} + O_2 \rightleftarrows \underset{\text{oxy}}{[Fe^{III}(\mu\text{-}O)Fe^{III}OOH^-]} \quad (16)$$

rather than the oxo bridge. Hydrogen bonding of this proton to the oxo bridge is indicated by resonance Raman studies.[111] In this respect the pioneering measurements of $-J$ for met- and oxyhemerythrin, 134 and 77 cm^{-1}, respectively,[112] have held up quite well qualitatively. The ^1H NMR results indicate that a ΔJ of 57 cm^{-1} between met and oxy is too large, however.[72]

The structural trans effect of the oxo bridge in complexes such as $[Fe_2O(OAc)_2(tmip)_2]^{2+}$ (Figure 3) has been noted. The protein crystal structure of highest resolution, that of azidometmyohemerythrin, also shows clear evidence for this structural trans effect.[109b] The trans Fe–N(Im) distances are more than 0.1 Å longer than the cis Fe–N(Im) distances. This structural trans effect in the synthetic models is greatly reduced when the oxo bridge is protonated.[32,51] Any assessment of the significance of this trans effect regarding reaction 16 must await sufficiently high resolution crystal structures of oxy- and deoxyhemerythrin.

In contrast to the synthetic (μ-oxo)bis(μ-carboxylato)diiron(III) complexes, the diiron site in methemerythrin will not exchange its oxo bridge with labeled solvent oxygen. Exchange is achieved only when the protein is reduced to the apparently more substitution-labile diferrous level.[111] This pattern of reactivity must reflect a lack of solvent access to the immediate vicinity of the diiron site. This lack of solvent access together with the acidity of the μ-hydroxo proton in tribridged diferric complexes[32,35] are the most likely reasons why the corresponding oxo-bridged structure is the one encountered in methemerythrin. The synthetic models so far isolated support the expectation that the proton on the hydroxo bridge of a diferrous complex would be less acidic than that on a diferric complex. This expectation is consistent with the pattern of bridging groups encountered in met- (oxo) and deoxyhemerythrin (hydroxo).

It is instructive to consider structural differences between pairs of related tribridged synthetic complexes. Either protonation of the oxo bridge or protonation of the bridge plus reduction of the iron atoms results in a 0.2–0.3-Å lengthening of the Fe···Fe distance.[30,32,51,52] The relevant comparisons of Fe···Fe distances are as follows: $[Fe_2O(OAc)_2(HB(pz)_3)_2]\cdot 4CH_3CN$ (3.145 Å) vs $[Fe_2(OH)(OAc)_2(HB(pz)_3)_2](ClO_4)\cdot 0.5CH_2Cl_2$ (3.439 Å); $[Fe_2O(OAc)_2(MTACN)_2](ClO_4)_2\cdot H_2O$ (3.12 Å) vs $[Fe^{II}_2(OH)(OAc)_2(MTACN)_2](ClO_4)_2\cdot H_2O$ (3.32 Å). EXAFS studies show that similar changes in Fe···Fe distance occur during redox changes of the diiron site in hemerythrin.[17,113,114] Because the ligands to the iron site are contributed by amino acid side chains, these changes in Fe···Fe distance must require adjustments by the surrounding protein. Since the reversible oxygenation of hemerythrin, reaction 16, involves formal redox changes of the iron atoms, such adjustments could also play a role in those oligomeric hemerythrins that show cooperativity in binding of O_2.[115]

2. Mixed-Valent Forms

As discussed in Magnetism, the protonation state of the mixed-valent iron site in hemerythrin has not been conclusively established; the $-J$ values are consistent with but do not prove the presence of a hydroxo bridge.[70,72] EXAFS studies show that the short (i.e., 1.8 Å) Fe–O(oxo) distance is absent in the azide adduct of semi-methemerythrin,[17] which is also consistent with a hydroxo bridge in this mixed-valent form. However, a comparison of Fe–O(oxo) distances in $[Fe(acen)]_2O$ vs $\{Na[Fe^{II,III}(acen)]_2O\}_2$ (Table I)[23,24] shows that protonation of the oxo bridge is *not* necessary for lengthening of the Fe–O(oxo) distances in a mixed-valent complex. The weakly coordinating sodium ion may partially compensate for the lack of a proton in this case, however. The available evidence on hemerythrin[70,114] suggests that protonation of the bridge is not a prerequisite for one-electron reduction of the diferric site in methemerythrin. Protonation *at some point* after one-electron reduction would be favored due to the expected increase in basicity of the oxo bridge. This protonation could remove thermodynamic and/or kinetic barriers to further reduction.

The potential for one-electron reduction of $[Fe_2O(OAc)_2(MTACN)_2]^{2+}$ (–0.37 V vs SCE) is more negative than that for reduction of the mixed-valent species to $[Fe^{II}_2(OH)(OAc)_2(MTACN)_2]^{+}$ (–0.29 vs SCE) in the presence of base, which implies that the $Fe^{II}Fe^{III}$ species is unstable with respect to disproportionation.[5,32] This fact represents one explanation for the inability (so far) to isolate the mixed-valent species. During controlled-potential coulometry it was found easier to stop at the mixed-valent species upon reduction of the (μ-oxo)diferric complex, than upon oxidation of the (μ-hydroxo)diferrous complex. This observation suggests that protonation of the oxo bridge is an essential prerequisite for either further reduction to the diferrous level or disproportionation. It is noteworthy in this latter regard that tribridged analogues in which the oxo bridge is replaced by a phenoxo bridge *can* be isolated as mixed-valent species.[82c,d] A similar line of reasoning can be applied to the oxygenation reaction 16. Transfer of the proton from the oxo bridge to the bound O_2, as shown in Figure 9, would facilitate two-electron rather than one-electron oxidation of the iron site. In the nitric oxide adduct of deoxyhemerythrin, the evidence indicates that the proton remains on the oxo bridge (cf. Figure 9), and at most, only one of the two iron atoms (Fe2) is oxidized.[116] Oxidations of deoxyhemerythrin by HONO[116,117] and by H_2O_2[118] support the idea that proton transfer from the hydroxo bridge facilitates two-electron oxidation of the iron site. The mixed-valent forms of the diiron site in hemerythrin disproportionate to varying extents and rates, either or both of which may be limited by protonation/deprotonation of the bridge.[70,92] Disproportionation and reduction of the mixed-valent oxidation level in hemerythrin may require valence detrapping,[70,82c] which could also be facilitated by protonation of the bridge. Isolation and characterization of (μ-oxo/hydroxo)bis(μ-carboxylato)diiron(II,III) synthetic models are needed for insight into these questions.

Finally, the behavior of the mixed-valent diiron site in hemerythrin may be contrasted with that in the purple acid phosphatases. The mixed-valent oxidation level of these phosphatases is enzymatically active and shows little or no tendency toward disproportionation.[74] On the basis of the preceding discussion, two possibilities suggest themselves: (i) The diiron site in purple acid phosphatases contains no oxo/hydroxo bridge. (There is currently no direct evidence for such a bridge.) (ii) The redox potentials of the diiron site in purple acid phosphatases differ from those for hemerythrin, because of phenoxo ligation to at least one of the iron atoms.[2,38]

C. Comparison of Hemerythrin and Methane Monooxygenase

Methane monooxygenase catalyzes the insertion of one atom of O_2 into methane, thereby producing

methanol according to reaction 17. Substrate oxidation occurs at the hydroxylase component of the enzyme, which contains a diiron center.[119] While the iron atoms

$$NADH + CH_4 + O_2 \rightarrow NAD^+ + CH_3OH + H_2O \quad (17)$$

in the diferric and mixed-valent oxidation levels of this center are known to be antiferromagnetically coupled,[92] the magnitude of coupling has not been established. Furthermore, the bridging groups and terminal ligands in this center have not been identified. The Mössbauer isomer shift for the diferric center in the hydroxylase (0.50 mm/s) indicates either 5- or 6-coordinate iron. The absorption spectrum of the diferric hydroxylase[119] is quite different from those of the synthetic oxo-bridged diferric complexes (Table II), and the Mössbauer quadrupole splitting for the diferric hydroxylase (1.07 mm/s)[92] is significantly smaller than for any of these synthetic complexes that contain one or two additional bridges. A hydroxo bridge plus one or more supporting bridges remains a possibility. The diferrous oxidation level of the hydroxylase is required for catalysis of oxygen insertion into methane and olefins.[119] The iron atoms of the diferrous site appear to be ferromagnetically coupled,[92] very much like those in the azide adduct of deoxyhemerythrin,[58] which was proposed to have an aqua bridge. A major roadblock to synthetic modeling of the hydroxylase chemistry is the relatively fragile nature of the reduced oxo/hydroxo-bridged diiron complexes. The use of appropriate dinucleating ligands may be a solution to this problem.[120] The reversible oxygenation of the diiron site in hemerythrin is best written as reaction 16.[110] The contrast with methane monooxygenase (reaction 17) is noteworthy: O_2 is believed to associate (at least transiently) with the diferrous cluster of the hydroxylase, but irreversible cleavage of the O–O bond is required. Diferrous complexes that reversibly bind O_2 and/or catalyze O_2 activation for hydroxylation of organic substrates represent perhaps the most prominent synthetic challenges in Fe–O–Fe chemistry.

Note Added in Proof. The X-ray crystal structure of the ribonucleotide reductase B2 subunit shows the (μ-oxo)(μ-carboxylato)diiron(III) core.[176]

XI. Acknowledgment

I thank Irving Klotz for first spurring my interest in this area. I thank Ji-Hu Zhang and Karl Hagen for help in the literature search and Sonia O'Dell for several drawings. I thank Dick Holm, Steve Lippard, Larry Que, Jr., Joann Sanders-Loehr, and Ed Solomon for preprints of manuscripts in advance of publication and for helpful discussions. Research in my laboratory referred to in this review has been supported by the National Institutes of Health. I am an NIH Research Career Development Awardee, 1988–1993.

Abbreviations

acac	acetylacetonate(1–)
acen	*N,N'*-ethylenebis(acetylacetone iminate)(2–)
ambp	$CH_3C[CH_2N{=}C(CH_3)CH_2C(CF_3)_2O]_2(CH_2NH_2)^{2-}$
bbmia	*N*-ethyl-*N,N*-bis(benzimidazol-2-ylmethyl)-amine
bbimae	2-[bis(benzimidazol-2-ylmethyl)amino]-ethanol
BIPhMe	bis(1-methylimidazol-2-yl)phenylmethoxy-methane
bipy	2,2'-bipyridine
bmen	2,2':6',2'':6'',2'''-tetrapyridine
btp	bis(*p*-tolyl) phosphide(1–)
cpbN	[(5-chloro-2-hydroxy-α-phenylbenzylidene)-amino]-1,5,9-triazanonane(2–)
Chel	4-hydroxy-2,6-pyridinedicarboxylate(2–)
CT	charge transfer
DAPDH	2,6-diacetylpyridine dioxime(1–)
DBAT	7,16-dihydro-6,8,15,17-tetramethyldibenzo-[*b,i*][1,4,8,11]tetraazacyclotetradecinate-(2–)
dipic	2,6-pyridinedicarboxylate(2–)
DMA-dipic	4-(dimethylamino)-2,6-pyridinedi-carboxylate(2–)
DMF	*N,N*-dimethylformamide
dmg	dimethylglyoxime
DMSO	dimethyl sulfoxide
DPDME	2,4-disubstituted deuteroporphyrin IX di-methyl ester(2–)
DSIT	*S*-methyl N^1,N^4-disalicylideneisothiosemi-carbazidate-S,N^1,N^4(2–)
dtne	1,2-bis(1,4,7-triaza-1-cyclononyl)ethane
EDTA	*N,N,N',N'*-ethylenediaminetetraacetate(4–)
en	ethylenediamine
EXAFS	extended X-ray absorption fine structure
FF	*N,N*-bis(5-*o*-phenyl-10,15,20-triphenyl-porphyrin)urea(4–)
$HB(pz)_3$	tris(1-pyrazolyl) hydroborate(1–)
hdp	*N*-(*o*-hydroxybenzyl)-*N,N*-bis(2-pyridyl-methyl)amine(1–)
hmb	2-hydroxy-3-methoxybenzaldoxime(1–)
hp	hemiporphyrazinate(2–)
Im	imidazole
IR	infrared
MCD	magnetic circular dichroism
MeH-XTA	*N,N'*-2-hydroxy-5-methyl-1,3-xylylenebis-[*N*-(carboxymethyl)glycine](5–)
4,4'-Me_2-bipy	4,4'-dimethyl-2,2'-bipyridine
mhq	2-methyl-8-hydroxyquinolinate(1–)
MPDP	*m*-phenylenedipropionate(2–)
MTACN	*N,N',N''*-trimethyl-1,4,7-triazacyclononane
N3	bis(benzimidazol-2-ylmethyl)amine
N5	*N,N,N'*-tris(benzimidazol-2-ylmethyl)-*N'*-(2-hydroxyethyl)-1,2-diaminoethane
N-base	imidazole, piperidine, pyridine, or 4-methylpyridine
NEtpy	*N*-ethylpyridinium
N-MeIm	*N*-methylimidazole
OAc	acetate(1–)
OBz	benzoate(1–)
ODM	5,15-dimethyl-2,3,7,8,12,13,17,18-octaethyl-porphyrinate(2–)
OEP	octaethylporphyrinate(2–)
OPr	propionate(1–)
mhq	2-methyl-8-hydroxyquinolinate(1–)
pbz	2-(2'-pyridyl)benzimidazole
P	generalized porphyrinate(2–)
Pc	phthalocyaninate(2–)
phen	1,10-phenanthroline

py	pyridine
sal	salicylaldoxime(1–)
salam	*N,N'*-ethylenebis(salicylamine)(2–)
salen	1,2-bis(salicylideneamino)ethane(2–)
salN-PhCl	*N*-(*p*-chlorophenyl)salicylaldimine(1–)
$(sal)_3$-trien	trisalicylidenetriethylenetetramine(3–)
Sq	squarate, $C_4O_4^{2-}$
TAAB	tetrabenzo[*b,f,j,n*][1,5,9,13]tetraazacyclohexadecine(2–)
TAAB-$(OMe)_2$	dimethoxide derivative of TAAB
TACN	1,4,7-triazacyclononane
5-*t*-Bu-salen	1,2-bis[(5-*tert*-butylsalicylidene)amino]ethane(2–)
3-*t*-Bu-salt-men	2,3-dimethyl-2,3-bis[(3-*tert*-butylsalicylidene)amino]butane(2–)
TDAD	17,18,19,20-tetrahydro-18,19-dioxotribenzo[*e,i,m*][1,4,8,11]tetraazacyclotetradecinate(2–)
tetpy	*N,N'*-bis(2-methylpyridyl)ethylenediamine
tetren	tetraethylenepentamine
tip	tris(imidazol-2-yl)phosphine
tmip	tris(*N*-methylimidazol-2-yl)phosphine
TMI-CMe	tris(1-methyl-2-imidazolyl)methoxymethane
TMpyP	*meso*-tetrakis(*N*-methyl-4-pyridyl)porphyrinate(2–)
tpa	tris(2-pyridylmethyl)amine
tpbn	tetrakis(2-pyridylmethyl)-1,4-butanediamine
TPC	7,8-dihydro-5,10,15,20-tetraphenylporphyrinate(2–)
TPP	*meso*-tetraphenylporphyrinate(2–)
TPPC	*meso*-tetrakis(4-carboxyphenyl)porphyrinate(2–)
TPP(4-CF_3)	*meso*-tetrakis[4-(trifluoromethyl)phenyl]porphyrinate(2–)
TPP(F_5)	*meso*-tetrakis(pentafluorophenyl)porphyrinate(2–)
TPP(4-OCH_3)	*meso*-tetrakis(4-methoxyphenyl)porphyrinate(2–)
$TPPS_4$	*meso*-tetrakis(4-sulfonatophenyl)porphyrinate(6–)
tptn	tetrakis(2-pyridylmethyl)-1,3-propanediamine
tsalen	1,2-bis(thiosalicylideneamino)ethane(2–)

Registry No. O_2, 7782-44-7; methane monooxygenase, 51961-97-8.

References

(1) Murray, K. S. *Coord. Chem. Rev.* **1974**, *12*, 1.
(2) (a) Que, L., Jr.; Scarrow, R. C. In *Metal Clusters in Proteins*; Que, L., Jr., Ed.; American Chemical Society: Washington, DC, 1988; p 302. (b) Sanders-Loehr, J. In *Iron Carriers and Iron Proteins*; Loehr, T. M., Ed.; VCH: New York, 1989; p 373.
(3) Armstrong, W. H.; Lippard, S. J. *J. Am. Chem. Soc.* **1983**, *105*, 4837.
(4) Wieghardt, K.; Pohl, J.; Gebrt, W. *Angew. Chem., Int. Ed. Engl.* **1983**, *22*, 727.
(5) (a) Lippard, S. J. *Angew. Chem., Int. Ed. Engl.* **1988**, *27*, 344. (b) Lippard, S. J. *Chem. Br.* **1986**, *22*, 222.
(6) West, B. O. *Polyhedron* **1989**, *8*, 219.
(7) Cotton, F. A.; Wilkinson, G. *Advanced Inorganic Chemistry*, 5th ed.; Wiley: New York, 1988; p 717.
(8) Greenwood, N. N.; Earnshaw, A. *Chemistry of the Elements*; Pergamon: New York, 1984; p 1265.
(9) Bridger, K.; Patel, R. C.; Matijevic, E. *J. Phys. Chem.* **1983**, *87*, 1192.
(10) Schneider, W. *Comments Inorg. Chem.* **1984**, *3*, 205.
(11) Khoe, G. H.; Brown, P. L.; Sylva, R. N.; Robins, R. G. *J. Chem. Soc., Dalton Trans.* **1986**, 1901.
(12) Morrison, T. I.; Reis, A. H., Jr.; Knapp, G. S.; Fradin, F. Y.; Chen, H.; Klippert, T. E. *J. Am. Chem. Soc.* **1978**, *100*, 3262.
(13) Magini, M.; Saltelli, A.; Caminiti, R. *Inorg. Chem.* **1981**, *20*, 3564.
(14) Morrison, T. I.; Shenoy, G. K.; Nielsen, L. *Inorg. Chem.* **1981**, *20*, 3565.
(15) Ou, C. C.; Wollman, R. G.; Hendrickson, D. N.; Potenza, J. A.; Schugar, H. J. *J. Am. Chem. Soc.* **1978**, *100*, 4717.
(16) Thich, J. A.; Ou, C.-C.; Powers, D.; Vasilious, B.; Mastropaolo, D.; Potenza, J. A.; Schugar, H. J. *J. Am. Chem. Soc.* **1976**, *98*, 1425.
(17) Scarrow, R. C.; Maroney, M. J.; Palmer, S. M.; Que, L., Jr.; Roe, A. L.; Salowe, S. P.; Stubbe, J. *J. Am. Chem. Soc.* **1987**, *109*, 7857.
(18) Hedman, B.; Co, M. S.; Armstrong, W. H.; Hodgson, K. O.; Lippard, S. J. *Inorg. Chem.* **1986**, *25*, 3708.
(19) Cai, J.; Lu, J. *Jiegou Huaxue* **1988**, *7*, 57.
(20) (a) Gomez-Romero, P.; DeFotis, G. C.; Jameson, G. B. *J. Am. Chem. Soc.* **1986**, *108*, 851. (b) Gomez-Romero, P.; Whitten, E. H.; Reiff, W. M.; Backes, G.; Sanders-Loehr, J. *J. Am. Chem. Soc.* **1989**, *111*, 9039.
(21) Collamati, I.; Dessy, G.; Fares, V. *Inorg. Chim. Acta* **1986**, *111*, 149.
(22) Gerloch, M.; McKenzie, E. D.; Towl, A. D. C. *J. Chem. Soc. A* **1969**, 2850.
(23) Corrazza, F.; Floriani, C.; Zehnder, M. *J. Chem. Soc., Dalton Trans.* **1987**, 709.
(24) Arena, F.; Floriani, C.; Chiesi-Villa, A.; Guastini, C. *J. Chem. Soc., Chem. Commun.* **1986**, 1369.
(25) Treichel, P. M.; Dean, W. K.; Calabrese, J. C. *Inorg. Chem.* **1973**, *12*, 2908.
(26) Drüeke, S.; Chaudhuri, P.; Pohl, K.; Wieghardt, K.; Ding, X.-Q.; Bill, E.; Sawaryn, A.; Trautwein, A. X.; Winkler, H.; Gurman, S. J. *J. Chem. Soc., Chem. Commun.* **1989**, 59.
(27) Mukherjee, R. N.; Stack, T. D. P.; Holm, R. H. *J. Am. Chem. Soc.* **1988**, *110*, 1850.
(28) Hay, J. P.; Thibeault, J. C.; Hoffman, R. J. *J. Am. Chem. Soc.* **1975**, *97*, 4884.
(29) Tatsumi, K.; Hoffman, R. *J. Am. Chem. Soc.* **1981**, *103*, 3328.
(30) Armstrong, W. H.; Spool, A.; Papaefthymiou, G. C.; Frankel, R. B.; Lippard, S. J. *J. Am. Chem. Soc.* **1984**, *106*, 3653.
(31) Spool, A.; Williams, I. D.; Lippard, S. J. *Inorg. Chem.* **1985**, *24*, 2156.
(32) Hartman, J. R.; Rardin, R. L.; Chaudhuri, P.; Pohl, K.; Wieghardt, K.; Nuber, B.; Weiss, J.; Papaefthymiou, G. C.; Frankel, R. B.; Lippard, S. J. *J. Am. Chem. Soc.* **1987**, *109*, 7387.
(33) Feng, X.; Bott, S. G.; Lippard, S. J. *J. Am. Chem. Soc.* **1989**, *111*, 8046.
(34) Wu, F.-J.; Kurtz, D. M., Jr. *J. Am. Chem. Soc.* **1989**, *111*, 6563.
(35) Wu, F.-J.; Kurtz, D. M., Jr.; Debrunner, P. G.; Nyman, P.; Hagen, K.; Vankai, V., submitted for publication in *Inorg. Chem.*
(36) Vincent, J. B.; Huffman, H. C.; Christou, G.; Li, Q.; Nanny, M. A.; Hendrickson, D. N.; Fong, R. H.; Fish, R. H. *J. Am. Chem. Soc.* **1988**, *110*, 6898.
(37) (a) Toftlund, H.; Murray, K. S.; Zwack, P. R.; Taylor, L. F.; Anderson, O. P. *J. Chem. Soc., Chem. Commun.* **1986**, 191. (b) Wieghardt, K.; Tolksdorf, I.; Herrmann, W. *Inorg. Chem.* **1985**, *24*, 1230.
(38) Yan, S.; Que, L., Jr.; Taylor, L. F.; Anderson, O. P. *J. Am. Chem. Soc.* **1988**, *110*, 5222.
(39) (a) Yan, S.; Cox, D. D.; Pearce, L. L.; Juarez-Garcia, C.; Que, L., Jr.; Zhang, J. H.; O'Connor, C. J. *Inorg. Chem.* **1989**, 28, 2507. (b) Norman, R. E.; Yan, S.; Que, L., Jr.; Backes, G.; Ling, J.; Sanders-Loehr, J.; Zhang, J. H.; O'Connor, C. J. *J. Am. Chem. Soc.* **1990**, *112*, 1554.
(40) Lloret, F.; Mollar, M.; Moratal, J.; Faus, J. *Inorg. Chim. Acta* **1986**, *124*, 67.
(41) Lloret, F.; Moratal, J.; Faus, J. *J. Chem. Soc., Dalton Trans.* **1983**, 1749.
(42) McLendon, G.; Motekaitis, R. J.; Martell, A. E. *Inorg. Chem.* **1976**, *15*, 2306.
(43) Miller, J. R.; Taies, J. A.; Silver, J. *Inorg. Chim. Acta* **1987**, *138*, 205.
(44) Goff, H.; Morgan, L. O. *Inorg. Chem.* **1976**, *15*, 3180.
(45) (a) Woon, T. C.; Shirazi, A.; Bruice, T. C. *Inorg. Chem.* **1986**, *25*, 3845. (b) More, K. M.; Eaton, G. R.; Eaton, S. S. *Inorg. Chem.* **1985**, *24*, 3698.
(46) (a) Chin, D.-H.; Balch, A. L.; La Mar, G. N. *J. Am. Chem. Soc.* **1980**, *102*, 1446. (b) Chin, D.-H.; La Mar, G. N.; Balch, A. L. *J. Am. Chem. Soc.* **1980**, *102*, 4344. (c) Balch, A. L.;

Chan, Y.-W.; Cheng, R.-J.; La Mar, G. N.; Latos-Grazynski, L.; Renner, M. W. *J. Am. Chem. Soc.* **1984**, *106*, 7779. (d) Latos-Grazynski, L.; Cheng, R.-J.; LaMar, G. N.; Balch, A. L. *J. Am. Chem. Soc.* **1982**, *104*, 5992.
(47) Holm, R. H. *Chem. Rev.* **1987**, *87*, 1401.
(48) Mockler, G. M.; deJersey, J.; Zerner, B.; O'Connor, C. J.; Sinn, E. *J. Am. Chem. Soc.* **1983**, *105*, 1891.
(49) (a) Gomez-Romero, P.; Casan-Pastor, N.; Ben-Hussein, A.; Jameson, G. B. *J. Am. Chem. Soc.* **1988**, *110*, 1988. (b) Nishida, Y.; Haga, S.; Tokii, T. *Chem. Lett.* **1989**, 109.
(50) Drüeke, S.; Wieghardt, K.; Nuber, B.; Weiss, J. *Inorg. Chem.* **1989**, *28*, 1414.
(51) Armstrong, W. H.; Lippard, S. J. *J. Am. Chem. Soc.* **1984**, *106*, 4632.
(52) Chaudhuri, P.; Wieghardt, K.; Nuber, B.; Weiss, J. *Angew. Chem., Int. Ed. Engl.* **1985**, *24*, 778.
(53) Armstrong, W. H.; Lippard, S. J. *J. Am. Chem. Soc.* **1985**, *107*, 3730.
(54) Turowski, P. N.; Armstrong, W. H.; Roth, M. E.; Lippard, S. J. *J. Am. Chem. Soc.* **1990**, *112*, 681.
(55) Sanders-Loehr, J.; Wheeler, W. D.; Shiemke, A. K.; Averill, B. A.; Loehr, T. M. *J. Am. Chem. Soc.* **1989**, *111*, 8084.
(56) Plowman, J. E.; Loehr, T. M.; Schauer, C. K.; Anderson, O. P. *Inorg. Chem.* **1984**, *23*, 3553.
(57) Solbrig, R. M.; Duff, L. L.; Shriver, D. F.; Klotz, I. M. *J. Inorg. Biochem.* **1982**, *17*, 69.
(58) Reem, R. C.; Solomon, E. I. *J. Am. Chem. Soc.* **1987**, *109*, 1216.
(59) Reem, R. C.; McCormick, J. M.; Richardson, D. E.; Devlin, F. J.; Stephens, P. J.; Musselman, R. L.; Solomon, E. I. *J. Am. Chem. Soc.* **1989**, *111*, 4688.
(60) Schugar, H. J.; Rossman, G. R.; Barraclough, C. G.; Gray, H. B. *J. Am. Chem. Soc.* **1972**, *94*, 2683.
(61) Lippard, S. J.; Schugar, H. J.; Walling, C. *Inorg. Chem.* **1967**, *6*, 127.
(62) Sanders-Loehr, J.; Loehr, T. M.; Mauk, A. G.; Gray, H. B. *J. Am. Chem. Soc.* **1980**, *102*, 6992.
(63) Czernuszewicz, R. S.; Sheats, J. E.; Spiro, T. G. *Inorg. Chem.* **1987**, *25*, 2063.
(64) Wing, R. M.; Callahan, K. P. *Inorg. Chem.* **1969**, *8*, 871.
(65) Martin, R. L. In *New Pathways in Inorganic Chemistry*; Ebsworth, E. A. V., Maddock, A. G., Sharpe, A. G., Eds.; Cambridge University Press: Cambridge, 1968; p 175.
(66) Earnshaw, A.; Lewis, J. *J. Chem. Soc.* **1961**, 376.
(67) (a) Wojciechowski, W. *Inorg. Chim. Acta* **1967**, *1*, 319. (b) *Ibid.* 324.
(68) O'Connor, C. J. *Prog. Inorg. Chem.* **1982**, *29*, 204.
(69) (a) Blake, A. B.; Yavari, A.; Hatfield, W. E.; Sekthulekshmi, C. N. *J. Chem. Soc., Dalton Trans.* **1985**, 2509. (b) Blake, A. B.; Yavari, A.; Kubicki, H. *J. Chem. Soc., Chem. Commun.* **1981**, 796.
(70) Pearce, L. L.; Kurtz, D. M., Jr.; Xia, Y.-M.; Debrunner, P. G. *J. Am. Chem. Soc.* **1987**, *109*, 7286.
(71) Dziobkowski, C. T.; Wrobleski, J. T.; Brown, D. B. *Inorg. Chem.* **1981**, *20*, 671.
(72) Maroney, M. J.; Kurtz, D. M., Jr.; Nocek, J. M.; Pearce, L. L.; Que, L., Jr. *J. Am. Chem. Soc.* **1986**, *108*, 6871.
(73) Lauffer, R. B.; Antanaitis, B. C.; Aisen, P.; Que, L., Jr. *J. Biol. Chem.* **1983**, *258*, 14212.
(74) Day, E. P.; David, S. S.; Peterson, J.; Dunham, W. R.; Bonvoison, J.; Sands, R. H.; Que, L., Jr. *J. Biol. Chem.* **1988**, *263*, 15561 and references therein.
(75) Helms, J. H.; Ter Haar, L. W.; Hatfield, W. E.; Tabitha, D.; Pemberton, J. E. *Inorg. Chem.* **1986**, *25*, 2334.
(76) Boersma, A. D.; Phillippi, M. A.; Goff, H. M. *J. Magn. Reson.* **1984**, *57*, 197.
(77) Strauss, S. M.; Pawlik, M. J.; Skowyra, J.; Kennedy, J. R.; Anderson, O. P.; Spartalian, K.; Dye, J. L. *Inorg. Chem.* **1987**, *26*, 724.
(78) Burke, J. M.; Kincaid, J. R.; Spiro, T. G. *J. Am. Chem. Soc.* **1978**, *100*, 6077.
(79) O'Keefe, D. H.; Barlow, C. H.; Smythe, G. A.; Fuchsman, W. H.; Moss, T. H.; Lilienthal, H. R.; Moss, T. H.; Caughey, W. S. *Bioinorg. Chem.* **1975**, *5*, 125.
(80) Robin, M. B.; Day, P. *Adv. Inorg. Chem. Radiochem.* **1967**, *10*, 247.
(81) Münck, E.; Papaefthymiou, V.; Sureus, K. K.; Girerd, J.-J. In *Metal Clusters in Proteins*; Que, L., Jr., Ed.; American Chemical Society: Washington, DC, 1988; p 302.
(82) (a) Snyder, B. S.; Patterson, G. S.; Abrahamson, A. J.; Holm, R. H. *J. Am. Chem. Soc.* **1989**, *111*, 5214. (b) Sureus, K. K.; Münck, E.; Snyder, B. S.; Holm, R. H. *J. Am. Chem. Soc.* **1989**, *111*, 5501. (c) Mashuta, M. S.; Webb, R. J.; Oberhausen, K. J.; Richardson, J. F.; Buchanan, R. M.; Hendrickson, D. N. *J. Am. Chem. Soc.* **1989**, *111*, 2745. (d) Borovik, A. S.; Papaefthymiou, V.; Taylor, L. F.; Anderson, D. P.; Que, L., Jr. *J. Am. Chem. Soc.* **1989**, *111*, 6183.
(83) Ginsberg, A. P. *Inorg. Chim. Acta Rev.* **1971**, *5*, 45.
(84) (a) Ercolani, C.; Rossi, G.; Monacelli, F. *Inorg. Chim. Acta* **1980**, *44*, L215. (b) Ercolani, C.; Gardini, M.; Monacellis, F.; Pessesi, G.; Rossi, G. *Inorg. Chem.* **1983**, *22*, 2584. (c) Ercolani, C.; Gardini, M.; Murray, K. S.; Pessesi, G.; Rossi, G. *Inorg. Chem.* **1986**, *25*, 3972.
(85) Kennedy, B. J.; Murray, K. S.; Zwack, P. R.; Homborg, H.; Kalz, W. *Inorg. Chem.* **1985**, *24*, 3302.
(86) Gorun, S. M.; Lippard, S. J. *Recl. Trav. Chim. Pays-Bas* **1987**, *106*, 417.
(87) Kahn, O.; Briat, B. *J. Chem. Soc., Faraday Trans. 2* **1976**, *72*, 1441.
(88) Sheats, J. E.; Czernuszewicz, R. S.; Dismukes, G. C.; Rheingold, A. L.; Petrouleas, V. L.; Stubbe, J.; Armstrong, W. H.; Beer, R. H.; Lippard, S. J. *J. Am. Chem. Soc.* **1987**, *109*, 1435.
(89) Wieghardt, K.; Bossek, U.; Nuber, B.; Weiss, J.; Bonvoisin, J.; Corbella, M.; Vitols, S. E.; Girerd, J. J. *J. Am. Chem. Soc.* **1988**, *110*, 7398.
(90) (a) Ercolani, C.; Gardini, M.; Murray, K. S.; Pennesi, G.; Rossi, G.; Zwack, P. R. *Inorg. Chem.* **1987**, *26*, 3539. (b) Bakshi, E. N.; Murray, K. S. *Hyperfine Int.* **1988**, *40*, 283.
(91) Wollman, R. G.; Hendrickson, D. N. *Inorg. Chem.* **1977**, *16*, 723.
(92) Fox, B. G.; Sureus, K. K.; Münck, E.; Lipscomb, J. D. *J. Biol. Chem.* **1988**, *263*, 10553.
(93) Kadish, K. M.; Larson, G.; Lexa, D.; Momenteau, M. *J. Am. Chem. Soc.* **1975**, *97*, 282.
(94) Esquivel, D. M. de S.; Ito, A. S.; Isotani, S. *J. Phys. Soc. Jpn.* **1976**, *40*, 947.
(95) Jezpwsla-Trzebiatowska, B.; Ozarowski, A.; Kozlowski, H.; Cukierda, T.; Hanuza, J. *J. Inorg. Nucl. Chem.* **1976**, *38*, 1447.
(96) Jezowska-Trzebiatowska, B.; Kozlowski, H.; Cukierda, T.; Ozarowski, A. *J. Mol. Struct.* **1973**, *19*, 663.
(97) (a) Chiari, B.; Piovesana, O.; Tarantelli, T.; Zanazzi, P. F. *Inorg. Chem.* **1983**, *22*, 2781. (b) Bailey, N. A.; McKenzie, E. D.; Worthington, J. M.; McPartlin, M.; Tasker, P. A. *Inorg. Chim. Acta* **1977**, *25*, L137.
(98) Borer, L.; Thalken, L.; Ceccarelli, C.; Glick, M.; Zhang, J. H.; Reiff, W. M. *Inorg. Chem.* **1983**, *22*, 1719.
(99) (a) Marini, P. J.; Murray, K. S.; West, B. O. *J. Chem. Soc., Chem. Commun.* **1981**, 726. (b) Marini, P. J.; Murray, K. S.; West, B. O. *J. Chem. Soc., Dalton Trans.* **1983**, 143.
(100) (a) Werth, W. T.; Kurtz, D. M., Jr.; Howes, B. D.; Huynh, B. H. *Inorg. Chem.* **1989**, *28*, 1357 and references therein. (b) Hendrich, M. P.; Debrunner, P. G. *Biophys. J.* **1989**, *56*, 489.
(101) Wenk, S. E.; Schultz, F. A. *J. Electroanal. Chem. Interfacial Electrochem.* **1979**, *101*, 89.
(102) (a) Chang, D.; Cocolius, P.; Wu, Y. T.; Kadish, K. M. *Inorg. Chem.* **1984**, *23*, 1629. (b) Phillipi, M. A.; Goff, H. M. *J. Am. Chem. Soc.* **1982**, *104*, 6026. (c) Hickman, D. L.; Nanthakumar, A.; Goff, H. M. *J. Am. Chem. Soc.* **1988**, *110*, 6384.
(103) (a) Bottomley, L. A.; Ercolani, C.; Gorce, J.-N.; Pennesi, G. *Inorg. Chem.* **1986**, *25*, 2338. (b) Ercolani, C.; Gardini, M.; Pennesi, G.; Rossi, G. *J. Chem. Soc., Chem. Commun.* **1983**, 549.
(104) (a) Peterson, M. W.; Richman, R. M. *Inorg. Chem.* **1985**, *24*, 722. (b) Perterson, M. W.; Rivers, D. S.; Richman, R. M. *J. Am. Chem. Soc.* **1985**, *105*, 2907. (c) Richman, R. S.; Peterson, M. W. *J. Am. Chem. Soc.* **1982**, *104*, 5795. (d) Bergamini, P.; Sostero, S.; Traverso, O.; Beplano, P.; Wilson, L. J. *J. Chem. Soc., Dalton Trans.* **1986**, 2311.
(105) Dicken, C. M.; Balasubramanian, P. N.; Bruice, T. C. *Inorg. Chem.* **1988**, *27*, 197.
(106) (a) Barton, D. H.; Boivon, J.; Gastiger, M.; Morzycki, J.; Hay-Motherwell, R. S.; Motherwell, W. B.; Ozbalik, N.; Schwartzentruber, K. M. *J. Chem. Soc., Perkin Trans. 1* **1986**, 947. (b) Barton, D. H. R.; Boivin, J.; Motherwell, W. B.; Ozbalik, N.; Schwartzentruber, K. M. *Nouv. J. Chim.* **1986**, *10*, 387.
(107) Murata, S.; Miura, M.; Nomura, M. *J. Chem. Soc., Chem. Commun.* **1989**, 116.
(108) Kitajima, N.; Fukui, H.; Moro-oka, Y. *J. Chem. Soc., Chem. Commun.* **1989**, 485.
(109) (a) Stenkamp, R. E.; Sieker, L. C.; Jensen, L. H. *J. Am. Chem. Soc.* **1984**, *106*, 618. (b) Sherrif, S.; Hendrickson, W. A.; Smith, J. L. *J. Mol. Biol.* **1987**, *197*, 273. (c) Sieker, L. C.; Stenkamp, R. E.; Jensen, L. H. In *The Biological Chemistry of Iron*; Dunford, H. B., Dolphin, D., Raymond, K. N., Sieker, L. C., Eds.; Reidel: New York, 1982; pp 161–175.
(110) Stenkamp, R. E.; Sieker, L. C.; Jensen, L. H.; McCallum, J. D.; Sanders-Loehr, J. *Proc. Natl. Acad. Sci. U.S.A.* **1985**, *82*, 713.
(111) (a) Shiemke, A. K.; Loehr, T. M.; Sanders-Loehr, J. *J. Am. Chem. Soc.* **1984**, *106*, 4951. (b) Shiemke, A. K.; Loehr, T. M.; Sanders-Loehr, J. *J. Am. Chem. Soc.* **1986**, *108*, 2437.
(112) Dawson, J. W.; Gray, H. B.; Hoenig, H. E.; Rossmann, G. R.; Schredder, J. M.; Wang, R. H. *Biochemistry* **1972**, *11*, 461.
(113) Zhang, K.; Stern, E. A.; Ellis, F.; Sanders-Loehr, J.; Shiemke, A. K. *Biochemistry* **1988**, *27*, 7470.

(114) Maroney, M. J.; Scarrow, R. C.; Que, L., Jr.; Roe, A. L.; Lukat, G. S.; Kurtz, D. M., Jr. *Inorg. Chem.* **1989**, *28*, 1342.
(115) Richardson, D. E.; Emad, M.; Reem, R. C.; Solomon, E. I. *Biochemistry* **1987**, *26*, 1003.
(116) Nocek, J. M.; Kurtz, D. M., Jr.; Sage, J. T.; Xia, Y.-M.; Debrunner, P.; Shiemke, A. K.; Sanders-Loehr, J.; Loehr, T. M. *Biochemistry* **1988**, *27*, 1014.
(117) Nocek, J. M.; Kurtz, D. M., Jr.; Pickering, R. A.; Doyle, M. P. *J. Biol. Chem.* **1984**, *259*, 12334.
(118) (a) Bradič, Z.; Harrington, P. C.; Wilkins, R. G. In *Biochemical and Clinical Aspects of Oxygen*; Caughey, W. S., Ed.; Academic Press: New York, 1979; p 459. (b) Armstrong, G. D.; Sykes, A. G. *Inorg. Chem.* **1986**, *25*, 3514.
(119) Fox, B. G.; Froland, W. A.; Dege, J. E.; Lipscomb, J. D. *J. Biol. Chem.* **1989**, *264*, 10023.
(120) Murch, B. P.; Bradley, F. C.; Que, L., Jr. *J. Am. Chem. Soc.* **1986**, *108*, 5027.
(121) (a) Davies, J. E.; Gatehouse, B. M. *Acta Crystallogr.* **1973**, *B29*, 1934. (b) *Ibid.* 2651.
(122) Wieghardt, K.; Pohl, K.; Bossek, U.; Nuber, B.; Weiss, J. *Z. Naturforsch.* **1988**, *B43*, 1184.
(123) (a) Jamenar, B.; Kaitner, B. *Cryst. Struct. Commun.* **1982**, *11*, 2043. (b) Kamenar, B.; Kaitner, B. In *Structural Studies of Molecules of Biological Interest*; Dodson, G., Glusker, J. P., Sayre, D., Eds.; Oxford University Press: London, 1981; p 123. (c) Katovic, V.; Vergez, S. C.; Busch, D. H. *Inorg. Chem.* **1977**, *16*, 1716.
(124) Vasilevsky, I.; Stenkamp, R. E.; Lingafelter, E. C.; Rose, N. J. *J. Coord. Chem.* **1988**, *19*, 171.
(125) Huang, L.; Jiang, F.; Lu, J. *Huaxue Tongbao* **1984**, 14.
(126) Bullen, G. J.; Howlin, B. J.; Silver, J.; Fitzsimmon, B. W.; Sayer, I.; Larkworthy, L. F. *J. Chem. Soc., Dalton Trans.* **1986**, 1937.
(127) Boeyens, J. C. A.; Khan, F. B. D.; Neuse, E. W. S. *Afr. J. Chem.* **1984**, *37*, 187.
(128) Carty, P.; Clare, K. C.; Creighton, J. R.; Metcalfe, E.; Raper, E. S.; Dawes, H. M. *Inorg. Chim. Acta* **1986**, *112*, 113.
(129) Petridis, D.; Terzis, A. *Inorg. Chim. Acta* **1986**, *118*, 129–134.
(130) Neuse, E. W.; Khan, F. B. D.; Berhalter, K.; Thewalt, U. *J. Crystallogr. Spectrosc. Res.* **1986**, *16*, 483.
(131) Zhou, K.; Huang, J. *Huaxue Tongbao* **1983**, 15.
(132) Weiss, H.; Straehle, J. *Z. Naturforsch.* **1984**, *39B*, 1453.
(133) Healy, P. C.; Skelton, B. W.; White, A. H. *Aust. J. Chem.* **1983**, *36*, 2057.
(134) Ponomarev, V. I.; Arutyunyan, L. D.; Atovmyan, L. O. *Kristallografiya* **1984**, *29*, 910.
(135) Reiff, W. R.; Witten, E. H.; Mottle, K.; Brennan, T. F.; Garafalo, A. R. *Inorg. Chim. Acta* **1983**, *77*, L83.
(136) Drew, M. G. B.; McKee, V.; Nelson, S. M. *J. Chem. Soc., Dalton Trans.* **1978**, 80.
(137) Dehnicke, K.; Prinz, H.; Massa, W.; Pebler, J.; Schmidt, R. *Z. Anorg. Allg. Chem.* **1983**, *499*, 20.
(138) Schmidbauer, H.; Zybill, C. E.; Negebauer, D. *Angew. Chem., Int. Ed. Engl.* **1983**, *22*, 156.
(139) Gomez-Romero, P.; Jameson, G. B. *J. Chem. Soc., Dalton Trans.* **1988**, 2747.
(140) Swepston, P. N.; Ibers, J. A. *Acta Crystallogr.* **1985**, *C41*, 671.
(141) Lay, K. L.; Buchler, J. W.; Kenny, J. E.; Scheidt, W. R. *Inorg. Chim. Acta* **1986**, *123*, 91.
(142) Landrum, J. T.; Grimmet, D.; Haller, K. J.; Scheidt, W. R.; Reed, C. A. *J. Am. Chem. Soc.* **1981**, *103*, 2640.
(143) Konefal, E.; Loeb, S. J.; Willis, C. J.; Stephan, D. W. *Inorg. Chim. Acta* **1986**, *115*, 147.
(144) Healy, P. C.; Patrick, J. M.; White, A. H. *Aust. J. Chem.* **1984**, *37*, 1405.
(145) Gozen, S. P. R.; Owston, P. G.; Tasker, P. A. *J. Chem. Soc., Chem. Commun.* **1980**, 1199.
(146) Weiss, M. C.; Goedken, V. L. *Inorg. Chem.* **1979**, *18*, 819.
(147) (a) Coda, A.; Kamenar, B.; Prout, K.; Carruthers, J. R.; Rollett, J. S. *Acta Crystallogr.* **1975**, *B31*, 1438. (b) Hanson, M. V.; Marsh, W. E.; Carlisle, G. O. *Inorg. Nucl. Chem. Lett.* **1977**, *13*, 277.
(148) Mabbs, F. E.; McLachlan, V. N.; McFadden, D.; McPhail, A. T. *J. Chem. Soc., Dalton Trans.* **1973**, 2016.
(149) Yampol'skaya, M. A.; Shova, S. G.; Gerbeleu, N. V.; Simonov, Y. A.; Bel'skii, V. K.; Dvorkin, A. A. *Sov. J. Coord. Chem.* **1983**, *28*, 984.
(150) Takahashi, K.; Nishida, Y.; Maeda, Y.; Kida, S. *J. Chem. Soc., Dalton Trans.* **1985**, 2375.
(151) Murch, B. P.; Bradley, F. C.; Boyle, P. D.; Papaefthymiou, V.; Que, L., Jr. *J. Am. Chem. Soc.* **1987**, *109*, 7993.
(152) Murch, B. P.; Boyle, P. D.; Que, L., Jr. *J. Am. Chem. Soc.* **1985**, *107*, 6728.
(153) Ou, C.-C.; Lalancette, R. A.; Potenza, J. A.; Schugar, H. J. *J. Am. Chem. Soc.* **1978**, *100*, 2053.
(154) Reiff, W. M.; Witten, E. H. *Polyhedron* **1984**, *3*, 443.
(155) Armstrong, W. H.; Lippard, S. J. *Inorg. Chem.* **1985**, *24*, 981.
(156) Do, Y.; Simhon, E. D.; Holm, R. H. *Inorg. Chem.* **1983**, *22*, 3809.
(157) Neuse, E. W.; Meirim, M. G. *Transition Met. Chem (Weinheim, Ger.)* **1984**, *9*, 205.
(158) Giannoccaro, P.; Pannacciulli, E.; Morazzoni, F.; Gervasini, A. *Gazz. Chim. Ital.* **1986**, *116*, 147.
(159) Kalz, W.; Homborg, H. *Z. Naturforsch.* **1983**, *B38*, 470.
(160) Kowalewski, P.; Merlin, J. C.; Bremard, C.; Moreau, S. *J. Mol. Struct.* **1988**, *175*, 55.
(161) Cerdonio, M.; Mogno, F.; Pispisa, B.; Romani, G. L.; Vitale, S. *Inorg. Chem.* **1977**, *16*, 400.
(162) Branca, M.; Pispisa, B.; Aurisicchio, C. *J. Chem. Soc., Dalton Trans.* **1976**, 1543.
(163) (a) Garg, V. K.; David, P. G.; Matsuzawa, T.; Shinjo, T. *Bull. Chem. Soc. Jpn.* **1975**, *48*, 1933. (b) David, P. G. *J. Inorg. Nucl. Chem.* **1973**, *45*, 1463.
(164) Buchler, J. W.; Schneehage, H. H. *Z. Naturforsch.* **1973**, *28B*, 433.
(165) Ghosh, S. P.; Mishra, L. K. *Inorg. Chim. Acta* **1973**, *7*, 545.
(166) Gerbeleu, N. V.; Shova, S. G.; Kuyavskaya, B. Y.; Turte, K. I.; Yampol'skaya, M. A.; Veksel'man, M. K. *Sov. J. Coord. Chem.* **1984**, *29*, 87.
(167) Wieghardt, K.; Pohl, K.; Ventur, D. *Angew. Chem., Int. Ed. Engl.* **1985**, *24*, 392.
(168) (a) Wrobleski, J. T.; Brown, D. B. *Inorg. Chim. Acta* **1979**, *35*, 109. (b) Wrobleski, J. T.; Brown, D. B. *Inorg. Chem.* **1978**, *17*, 2529. (c) Long, G. H. *Inorg. Chem.* **1978**, *17*, 2702.
(169) Rani, I.; Pandeya, K. B.; Sawhney, G. L.; Baijal, J. S. *Acta Chim. Acad. Sci. Hung.* **1982**, *110*, 75.
(170) Collamati, I.; Cervone, E. *Inorg. Chim. Acta* **1986**, *123*, 147.
(171) Adler, J.; Ensling, J.; Gütlich, P.; Bominaar, E. L.; Gullin, J.; Trautwein, A. X. *Hyperfine Int.* **1988**, *42*, 869.
(172) Beer, R. H.; Tolman, W. B.; Bott, S. G.; Lippard, S. J. *Inorg. Chem.* **1989**, *28*, 4559.
(173) Tolman, W. B.; Bino, A.; Lippard, S. J. *J. Am. Chem. Soc.* **1989**, *111*, 8522.
(174) Drüeke, S.; Wieghardt, K.; Nuber, B.; Weiss, J.; Fleischauer, H.-P.; Gehring, S.; Haase, W. *J. Am. Chem. Soc.* **1989**, *111*, 8622.
(175) Bossek, U.; Weyhermüller, T.; Wieghardt, K.; Bonvoisin, J.; Girerd, J. J. *J. Chem. Soc., Chem. Commun.* **1989**, 633.
(176) Nordlund, P.; Sjöberg, B.-M.; Eklund, H. Submitted for publication in *Nature*.